PROGRESS REPORT
Grant NGR-34-002-047/S2
February 15, 1968

"STUDY OF RECTANGULAR-GUIDE-LIKE STRUCTURES FOR MILLIMETER WAVE TRANSMISSION"

to
The National Aeronautics and Space Administration, Washington, D. C.

DEPARTMENT OF ELECTRICAL ENGINEERING
NORTH CAROLINA STATE UNIVERSITY
RALEIGH, NORTH CAROLINA

PROGRESS REPORT
Grant NGR-34-002-047/S2
February 15, 1968

"STUDY OF RECTANGULAR-GUIDE-LIKE STRUCTURES FOR MILLIMETER WAVE TRANSMISSION"

to
The National Aeronautics and Space Administration, Washington, D. C.

North Carolina State University
Raleigh, North Carolina

Submitted: Frederick J. Tischer

Dr. Frederick J. Tischer, Professor
Principal Investigator

PERSONNEL

Dr. Frederick J. Tischer, Principal Investigator

Mr. A. T. Shankle, Research Assistant

Mr. J. J. Pan, Research Assistant

Mr. I. H. Chen,* Graduate Student

Mr. R. Packard, Undergraduate Assistant

Messrs. R. Carpenter and L. Young**

* Mr. Chen is a Ph.D. candidate carrying out studies of beam waveguides for millimeter-wave transmission and related surface-loss effects of reflectors.

** These two students have completed a study of the effects of losses of wire grids as a part of the departmental honors program.

TABLE OF CONTENTS

INTRODUCTION

This progress report presents the results of research carried out under Grant NGR 34-002-047/S2 during the period October 1, 1968 to January 31, 1968.

The progress report consists of several parts dealing with various topics of millimeter-wave transmission by unconventional guidance principles. One of the parts deals with measurements of the attenuation and Q-values of waveguide sections with artificial dielectrics carried out at 35 GHz. Two subsequent parts deal with the fence guide; one of them with measurements of the loss characteristics of thick wire grids and the other with a proposal of a low-leakage fence-guide structure. A fourth part presents computer programs for obtaining graphs for the attenuation of single-slab H-guides in terms of the structural dimensions.

The preceding theoretical studies of the H-guide with artificial dielectrics have shown that reductions of the attenuation of H-guides made possible by the use of artificial dielectrics in the form of high-permittivity dielectric strips and metallic-strip structures represent a significant improvement of the characteristics of this type of waveguides. The measurements at 35 GHz preliminarily confirm these findings. A more thorough evaluation of the results is in progress at present. The primary purpose of the measurements, however, was to gain information required for the design of a prototype model of an H-guide with metallic strip structure which will be used

for the comparison of the various design approaches of rectangular-guide-like structures.

Measurements of the characteristics of thick-wire grids are described next which were carried out during the report period to verify the validity of relationships used for their computation. The measured values of the reflection and transmission coefficients of lossy-wire grids are compared with computed values. Wire grids made of brass and silver-plated wires are considered. Satisfactory agreement was obtained for small spacing, particularly important for the design of grids for fence-guide application. As a supplement, a method was developed for the computation of the characteristics of grids composed of rectangular posts. The results are under evaluation at present.

In the third part of this report, a new concept in fence-guide design is outlined. The concept is based on the fact that the leakage of energy through the wire grid depends on the ratio of the phase velocity of waves in the waveguide to that of waves radiated from the wire grid. It can be shown that the leakage becomes negligible when the ratio approaches or is less than one. Reduction of this ratio can be achieved by dielectric loading of the internal region of the fence guide. Several examples for structures by which this can be accomplished are shown.

A presentation of revised relationships and graphs of the attenuation of single-slab waveguides concludes the report.

The contributions to the attenuation by the wall losses and the dielectric losses are presented graphically in terms of the dielectric slab thickness and plate separation in normalized form. By the normalization, some of the results become frequency-independent.

Q-VALUE MEASUREMENTS ON SHORTENED H-GUIDE TEST SECTIONS

Abstract

Q-value measurements on shortened H-guide test sections forming a cavity are described. The rectangular cavity contains centrally located guiding structures such as dielectric slabs or metallic strip structures. The Q-value measurements actually represent measurements of the attenuation of the shortened waveguide sections. The reported measurements were carried out at 35 GHz.

The measurement setup, the measurement procedures, and results are described. Emphasis was placed on the measurement of the characteristics of an H-guide with artificial dielectric in the form of a metallic-strip structure. To facilitate comparisons, the characteristics of guides with dielectric slabs and of commercially available rectangular guides were determined also.

Some nonconventional phases of the measurement procedure, such as frequency measurement of the swept-frequency signal, mode analysis and mode identification, and improvements of the accuracy of the actual Q-value determination are discussed in greater detail.

Introduction

Q-value measurements of H-guide test sections with various guiding structures were carried out to verify the results obtained previously by computation. Verification of computed values of attenuation and Q is necessary in the millimeter-wave region since considerable discrepancies are usually observed in this frequency range. The discrepancies are the result of differences between the measured and computed values of the surface resistance if the bulk values of conductivity of the material of the walls are used in the computation.

An additional purpose of the Q-value measurement is the determination of the data of dielectrics which are to be used in design of H-guide structures with artificial dielectrics. The maximum frequency for which their data are usually furnished by the manufacturer is 10 GHz. Considerable differences were observed between these data and those at millimeter waves in the 35 GHz region.

The measurements of the characteristics of the various guiding structures usually consist of two parts, a mode analysis of the cavity after insertion of the structure and the actual Q-value determination. The mode analysis is necessary to identify the H-guide modes among the spectrum of frequencies at which the cavity resonates. If several resonances are observed in the frequency region where the H-guide mode is supposed to be located, mode suppressors have to be used to eliminate the undesired mode

or to dislocate their resonant frequencies. Thin wires, oriented and located at appropriate places in the cavity were tested as mode modifiers and found useful for the frequency dislocation of interfering modes. Absorbing layers inserted into the cavity were found to be the most effective means of mode suppressors. Layers of paper and cardboard of varying thicknesses served as absorbers.

For the determination of the resonant-frequency spectrum, the use of a calibrated cavity-type frequency meter was found unsatisfactory due to its low Q-value. Heterodyne frequency measurement has to be used for this purpose and for the Q-value measurements. The frequency measurement is described in one of the sections of this report.

The preliminary measurements described in the preceding progress report (October 15, 1968) dealt primarily with the mode analysis. However, Q-value measurements were also carried out at that time to determine whether the errors resulting from the instruments and from the measurement procedures were sufficiently low to give meaningful results. It was found that this was not the case and improvements were necessary to obtain satisfactory accuracy and repeatability. A description of the improvements is also a part of this report.

The content of the report consists of a brief description of the measurement setup used for the mode analysis, Q-value measurement, and the determination of the insertion loss (for finding the unloaded Q-value). The heterodyne frequency measurement described in one of the following sections represents an

important part of the measurement operation. The actual Q-value determination is described in the following sections on wave mode identification, Q-value measurement, and in Appendix A. The measurement results are presented in the following sections for dielectric slabs, metallic strip structures, and in Appendix B for rectangular waveguides. The measured results then facilitate comparisons of the measured values of Q and attenuation of rectangular standard waveguides, H-guides with dielectric slabs, and H-guides with artificial dielectrics in the form of metallic-strip structures. Evaluation of the measured data is being carried out at present.

General Description of the Measurement Setup

The setup developed for the millimeter wave measurements basically serves two purposes: One is to determine and to identify the various wave modes which can be excited when various types of structures are inserted into the test cavity. The structures are to be used later for waveguides. The second purpose is to measure the Q-value for the identified H-guide modes. From it, the values of attenuation of the waveguides containing the corresponding structures are found. The circuitry has been described in a previous report of October 15, 1968, however, it was somewhat modified and the measurements were refined to improve the accuracy of the determination of the Q-values. A circuit diagram is shown in Fig. 1.

The setup consists of two major parts. The first part includes a 35 GHz klystron as a power source which is frequency modulated by applying to the repeller a sawtooth voltage obtained from the deflection circuit of the oscilloscope. The energy of the klystron is fed through an isolator, attenuator, two directional couplers, a precision attenuator, and a second isolator into the test cavity. The output of the cavity is connected through an E,H-tuner and a variable attenuator with the detector. The DC output of the detector is fed into Channel A of the oscilloscope. The oscilloscope is a dual-beam, differential-input, Hewlett-Packard Model 132A.

The second part includes two branches of which one provides rough determination of the frequency by a cavity-type, calibrated

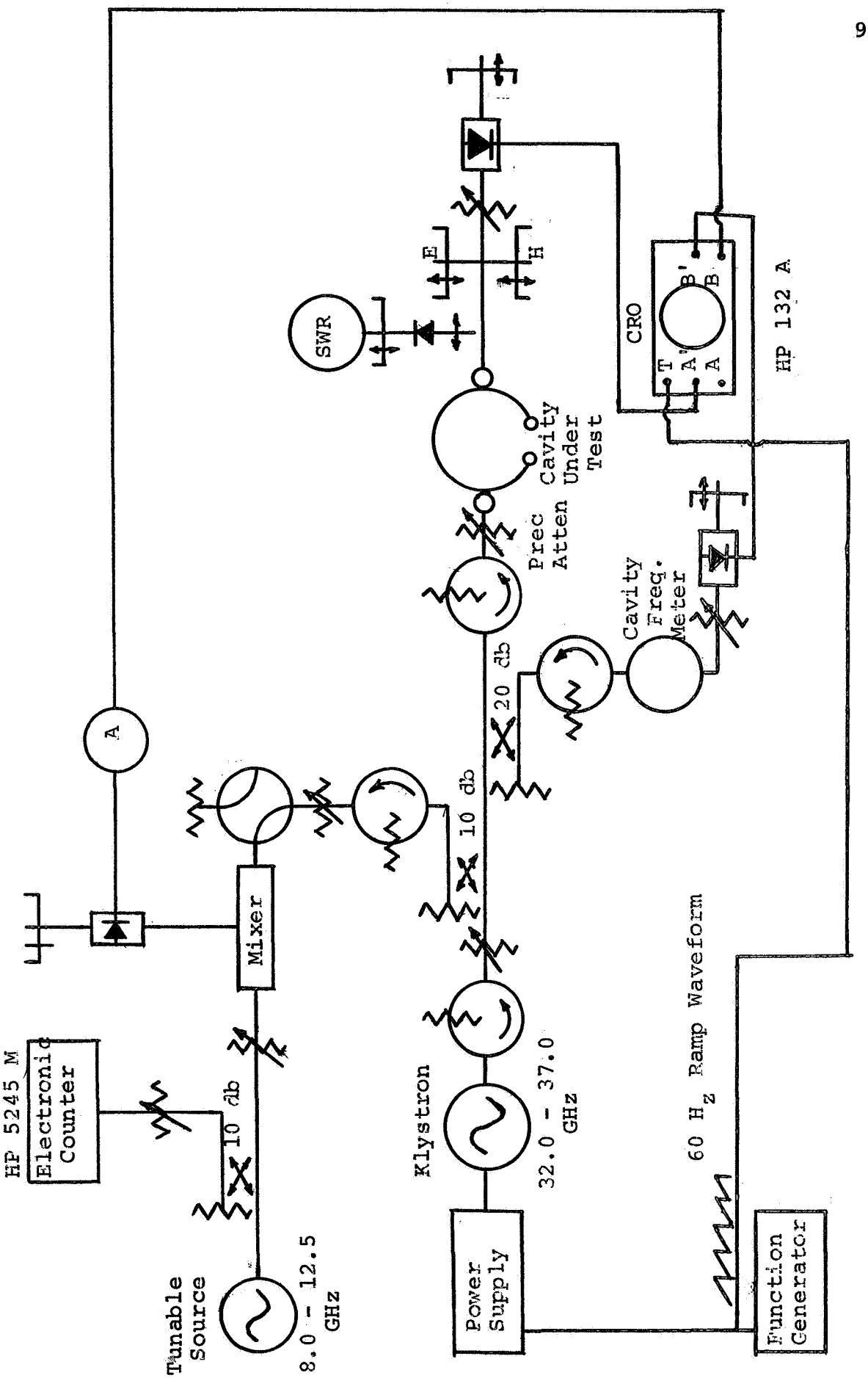

Fig. 1 Skematic diagram of the test circuit

frequency meter and a signal which is proportional to the output amplitude of the klystron. The latter signal is applied to Channel B+ of the oscilloscope and is used to determine the transfer ratio of the test cavity and to give a reference signal for the Q-value measurement. The other branch feeds the A-band signal into a mixer which in combination with a tunable X-band signal yields a heterodyne beat signal of the difference frequency between the fourth harmonic of the signal of the X-band oscillator and the A-band signal. Presence of the beat signal is used for the calibration of the oscilloscope graticule for the swept-frequency signal of the klystron. A low-pass filter is inserted into the line which feeds the amplfied output signal of the mixer to Channel B- of the oscilloscope.

Swept-Frequency Operation

A 60-cycle sawtooth signal made available from a function generator or from the deflection circuit of the oscilloscope is superimposed to the repeller voltage for the A-band klystron and simultaneously applied to the horizontal deflection of the Hewlett-Packard Model 132A, dual-beam, differential-input oscilloscope. The output frequency of the klystron is within a limited region proportional to the magnitude of the repeller voltage. Therefore, by applying a ramp, or sawtooth, waveform to the repeller, the output frequency of the klystron varies linearly with time over a narrow frequency band. Adjustment of the magnitude of the ramp waveform controls the range of the frequency sweep. Applying this same waveform to the horizontal deflection, the oscilloscope

displays the observed quantity as a function of frequency. The swept-frequency operation is then used for the mode identification and the Q-value measurement.

Heterodyne Frequency Measurement

A small portion of the swept A-band signal is sampled through a 10 db directional coupler transmitted through a variable attenuator and used as an input to the A-band port of a De Mornay Bonardi DBGD-350 Crystal Multiplier. Energy from an X-band tunable source (a Hewlett-Packard Sweep Oscillator is being used at the present time), the frequency of same being continuously monitored through a 10 db directional coupler and variable attenuator by a Hewlett-Packard 5245M Electronic Counter, is used as an input, through a variable attenuator, to the X-band port of the multiplier. The multiplier consists of adjustable shorts in both the A and X band arms and a 1N53 crystal diode properly located and coupled into the circuit so that the low-frequency output signal of the multiplier, which in effect is a resonant cavity, can be detected. Detectable mixing occurs when the A-band frequency equals a convenient harmonic; e.g., the fourth harmonic, of the X-band frequency. When this condition is fulfilled, a spike in the low-frequency output of the mixer occurs. This spike is amplified, filtered, and R-C coupled into Channel B- of the oscilloscope. The relative positions of the movable shorts is adjusted such that the output of the 1N53 is a maximum and unwanted harmonically related signals are reduced. The frequency of the A-band signal can then be found monitoring the X-band signal with the frequency counter and by

multiplying the counter frequency by the harmonic multiplication factor (4) for the frequency that has been utilized. This technique for the accurate determination of A-band frequencies has been quite successful and has resulted in frequency measurements having a relative error of about $\pm$0.003%.

Wave Mode Identification

Since a number of wave modes are excited in the test cavity, including the H-guide modes under investigation and other undesired modes, a careful identification of the observed resonances has to be carried out. As a first step, the resonance frequencies of all modes are determined. A calibrated resonant-cavity frequency meter gives a rough indication of the frequency, which afterward is measured accurately by the heterodyne circuit. The separation of the wave modes into those of the H-guide type and the undesired modes is done, at present, by inserting absorbing layers of material on the top and bottom of the cavity. Other methods of mode filters were tested before but did not give the desired results. The absorbing material introduces losses and attenuates the undesired cavity modes considerably, but has very little effect on the H-guide modes since their fields decay exponentially toward the top and bottom walls of the cavity where the absorbing layers are located. Absorbing layers of three thicknesses have been applied. For the identification of the wave modes, the transfer ratio, which is the ratio of output to input signal of the test cavity, is observed. The transfer ratio is a rough indication of the Q-value. The Q-values of the cavity

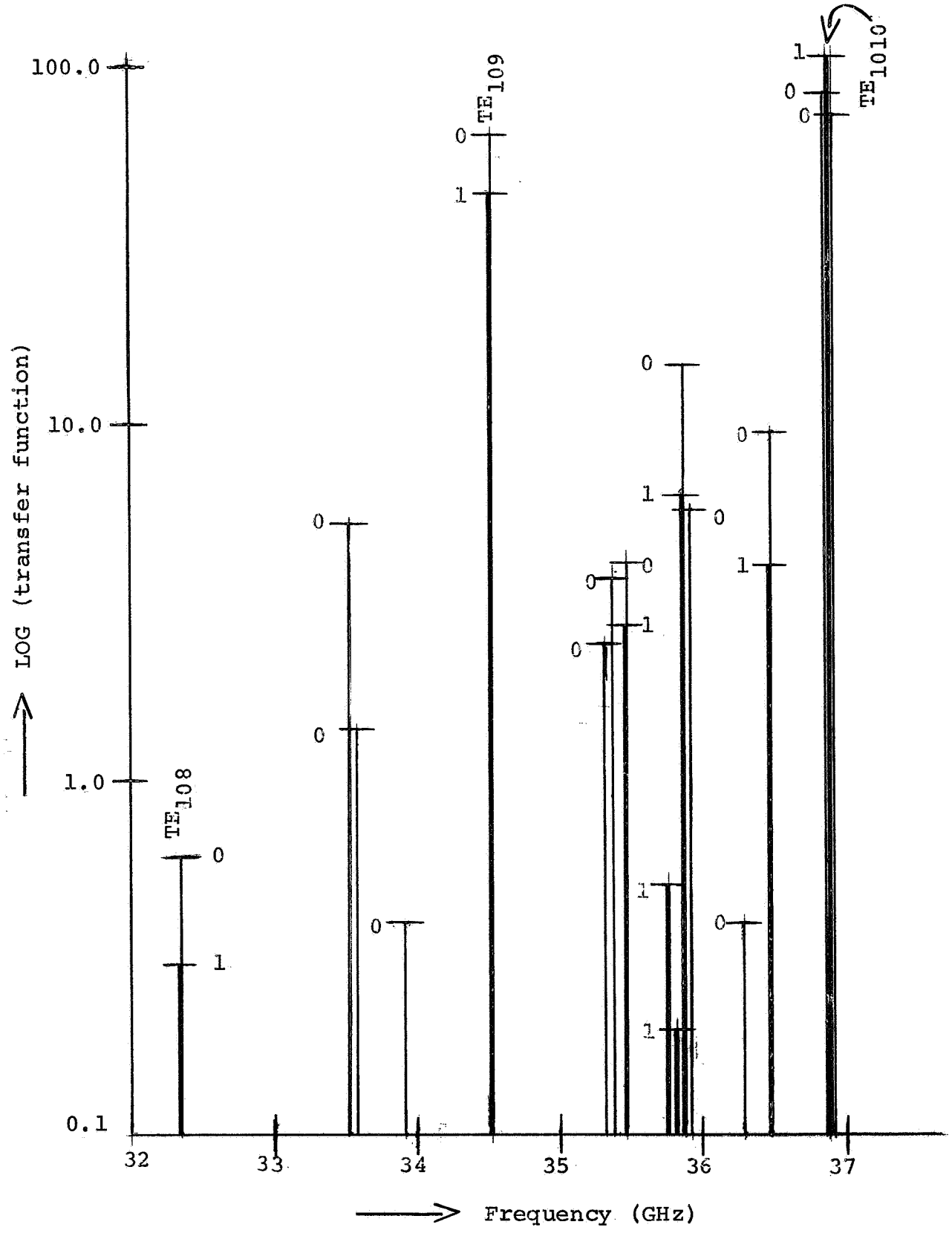

Legend: 0, magnitude, no abs. layers
1, magnitude, AL1 inserted

Fig. 2 Mode and transfer ratio spectrum for the 0.85 mm Rexolite H-guide

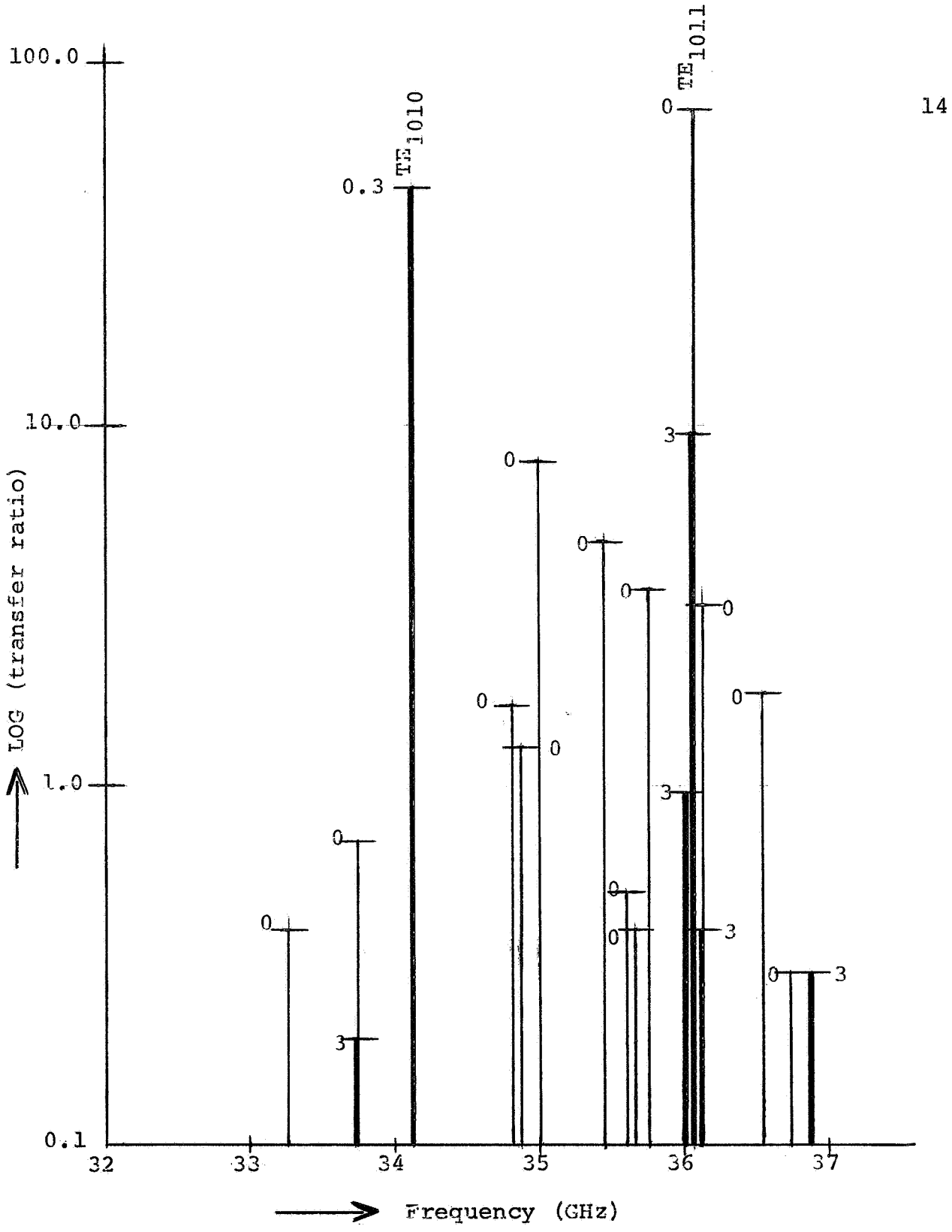

Legend: 0, magnitude, no abs. layers
3, magnitude, AL3 inserted

Fig. 3 Mode and transfer ratio spectrum for the 1.955 mm-slab H-guide

for H-guide modes is only slightly affected by the absorbing layers and is characterized by low-transfer ratios. The procedure makes possible the identification of the H-guide modes. Figs. 2 and 3 show the magnitudes of the transfer ratio for the various wave modes without and with various absorbing layers (denoted by AL1 and AL3) inserted. The characteristics of the absorbing layers are:

AL1: Thickness 0.15 mm, typewriter bond paper

AL2: Thickness 0.35 mm, heavy paper

AL3: Thickness 0.65 mm, cardboard

Moderate reduction of the magnitudes of the transfer ratio is typical for the H-guide modes.

Improved Method of Q-Value Measurement

Preceding measurements of the Q-values in the millimeter wave region have shown that excessive discrepancies existed between measured and computed values and that the repeatability of the measurements was not satisfactory. For this reason, a new cavity made of solid copper, highly polished before assembly, was manufactured and is used for the present measurements. The repeatability was additionally improved by using steel screws and by careful assembly procedures. Further improvement of the accuracy of the Q-value measurement was obtained by taking into account the variation of the output amplitude of the klystron during the frequency sweep. This problem did not exist at X-band frequencies since a leveled frequency-sweep generator was used. The non-leveled output of the klystron is taken into account by

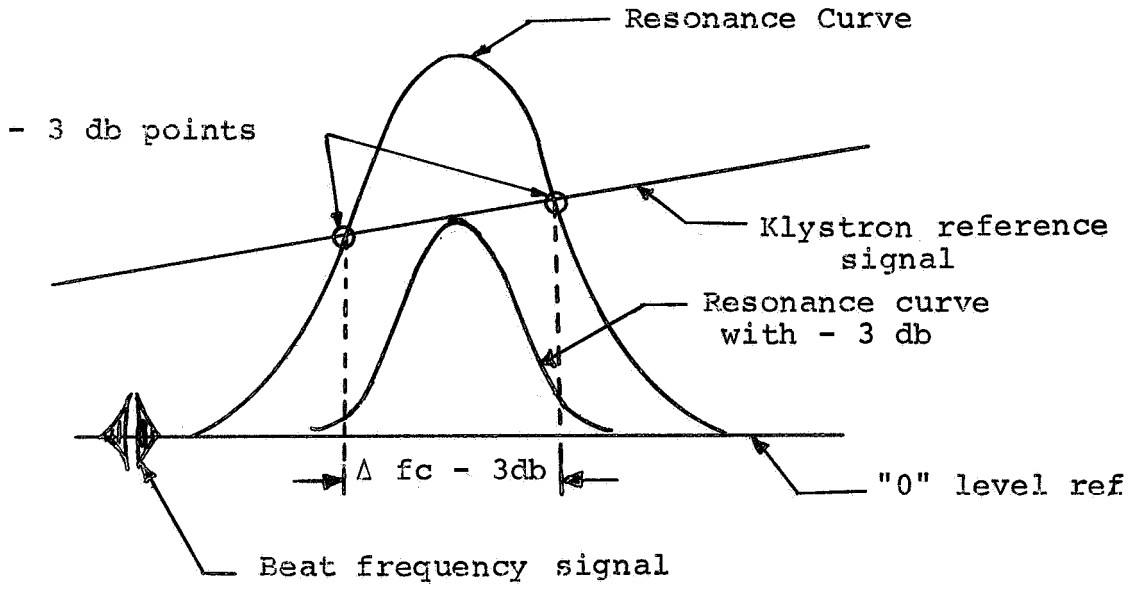

Fig. 4 Oscilloscope display for Q-value measurement

using the second trace of the oscilloscope as a reference level. This trace shows on the oscilloscope the varying output level centered at 3 db below the maximum of the other trace which describes the resonance curve as shown in Fig. 4. The Q-value is obtained by determining the frequencies where the reference trace intersects the trace representing the resonance curve of the cavity. For the determination of the frequencies at the intersection points, the graticule of the oscilloscope is calibrated at the beginning of the measurement by the use of the heterodyne frequency technique described in one of the preceding sections. It should be noted that the error of the frequency determination is less than $\pm$1 MHz at 35 GHz. Improvement of the measurement accuracy was also obtained by limiting the measurement region on the oscilloscope to the linear portion of the graticule of the oscilloscope.

Q-Value Measurement for Dielectric Slabs

The Q-value of the cavity was measured after insertion of dielectric slabs of varying thicknesses for obtaining reference values for the later measurements on artificial dielectrics. The thicknesses used were 0.85, 1.435, 1.955, and 2.55 mm. A mode analysis and identification similar to that described earlier was carried out as a first step. The measurement data are presented in Figs. 2, 3, and 5. Plots of the transfer ratios in logarithmic scale vs. resonant frequency are shown in Figs. 2 and 3. The lengths of the light lines indicate the ratios after insertion of the dielectric slabs of specified thicknesses. The

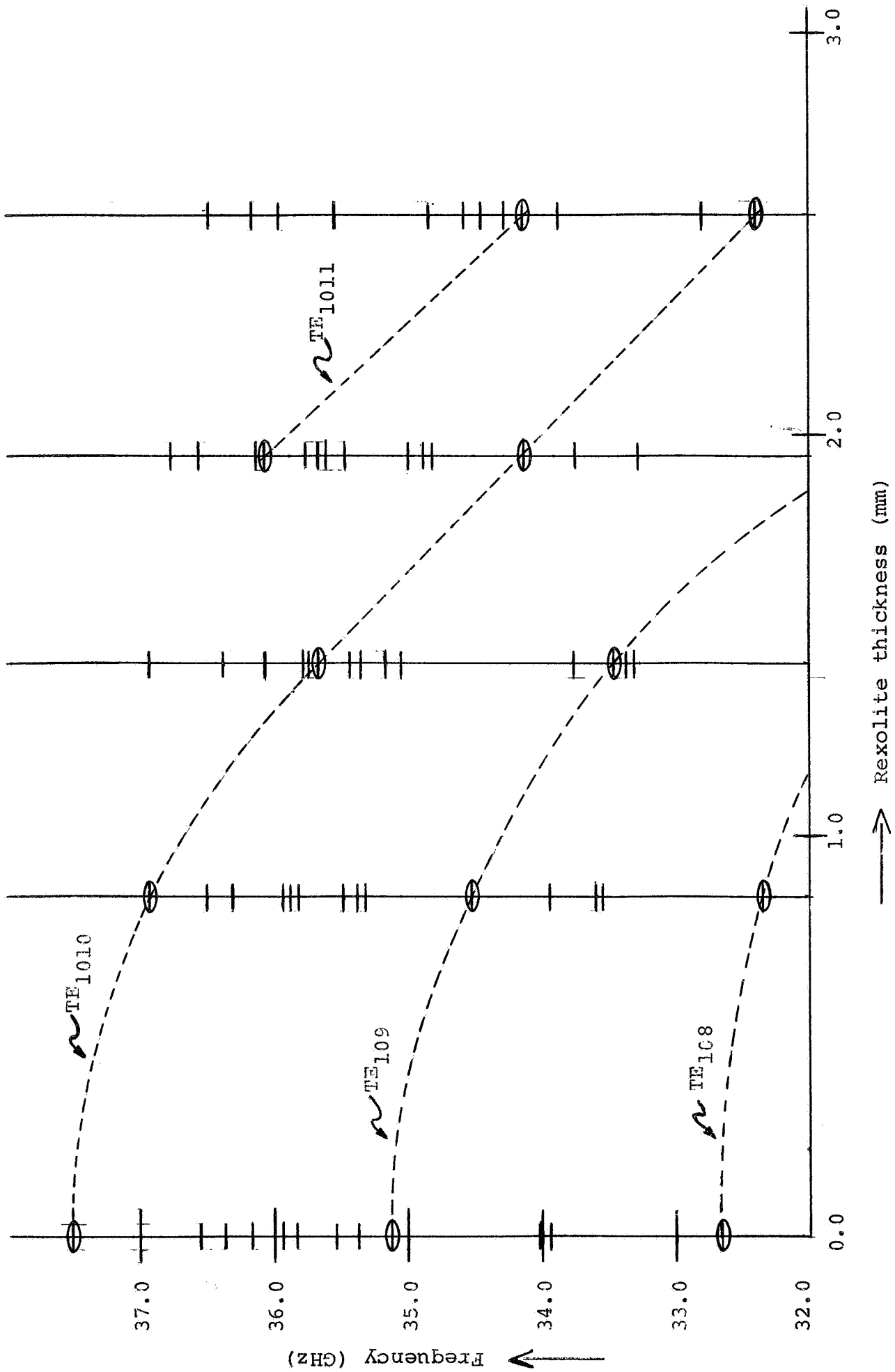

Fig. 5 Mode spectra of the cavity and frequency shifts of H-guide modes for various thicknesses of the dielectric slabs

values reduced by the losses in the absorbing layers (AL1 and AL3) are indicated by heavier lines and the added number 1 to 3. The number 1 indicates the reduced amplitude after insertion of the absorbing layer AL1, and so on. Plots for 0.85 and 1.955 mm Rexolite are shown. As indicated by the graphs, the H-guide modes TE_{10n} are only slightly affected by the presence of the lossy layers on the top and bottom surfaces of the cavity. The ratios for the other wave modes are reduced appreciably and some fall below the observable level. Based on this procedure, the H-guide modes TE_{109}, TE_{1010}, and TE_{1011} were identified. The graph of Fig. 5 shows the mode spectra for each thickness of the dielectric slab and the shifts of the resonance frequencies for the identified TE_{10n} modes by the dashed lines. The graph can be used for the determination of the values of the guide wavelength of H-guide modes for the specified thicknesses of the dielectric slabs and for their comparison with the theoretical values. It is noted that the TE_{10n} H-guide modes are actually hybrid modes with longitudinal components of the electric and magnetic fields.

As a next step, the Q-values, loaded and unloaded, were determined. The loaded Q-values were measured by the described method. Measurements and relationships for finding the unloaded Q-values are described in Appendix 1. Table 1 provides a listing of the Q's obtained for the different thicknesses of slabs for the H-guide modes that were identified. The data show that with increasing thicknesses of the slab, the Q-values decrease due to

Table 1

Slab Thickness	LOADED Q			UNLOADED Q		
	TE_{109}	TE_{1010}	TE_{1011}	TE_{109}	TE_{1010}	TE_{1011}
0.85 mm	(34.550) 8345	----	----	8867	----	----
1.435 mm	(33.493) 5409	(35.675) 5170	----	5832	5841	----
1.955 mm	----	(34.180) 2790	(36.126) 2970	----	2956	3332
2.55 mm	----	(32.452) 2760	(34.209) 1941	----	2924	1976

dielectric losses in the slabs. It should be noted that the maximum error of the Q-value measurements is about $\pm$500 in the absence of interfering wave modes. The obtained Q-values can then be used for the determination of the attenuation of the H-guide. The method of the evaluation and the results will be discussed later.

Q-Value for Metallic Strip Structure

A modal analysis was performed on both strip structures to identify the TE_{10n} modes of resonance. At the insertion of the absorbing layers, the transfer ratios for other than H-guide modes for the wide strip structure was considerably affected as indicated in Fig. 6. The figure shows the transfer ratios for the wave modes at specific frequencies by the lengths of the vertical lines. The medium lines stand for the ratios after insertion of the absorbing layers No. 2 (AL2). For AL3 only two wave modes were observable and are indicated by the heavy line. This permitted identification of the H-guide modes for this structure.

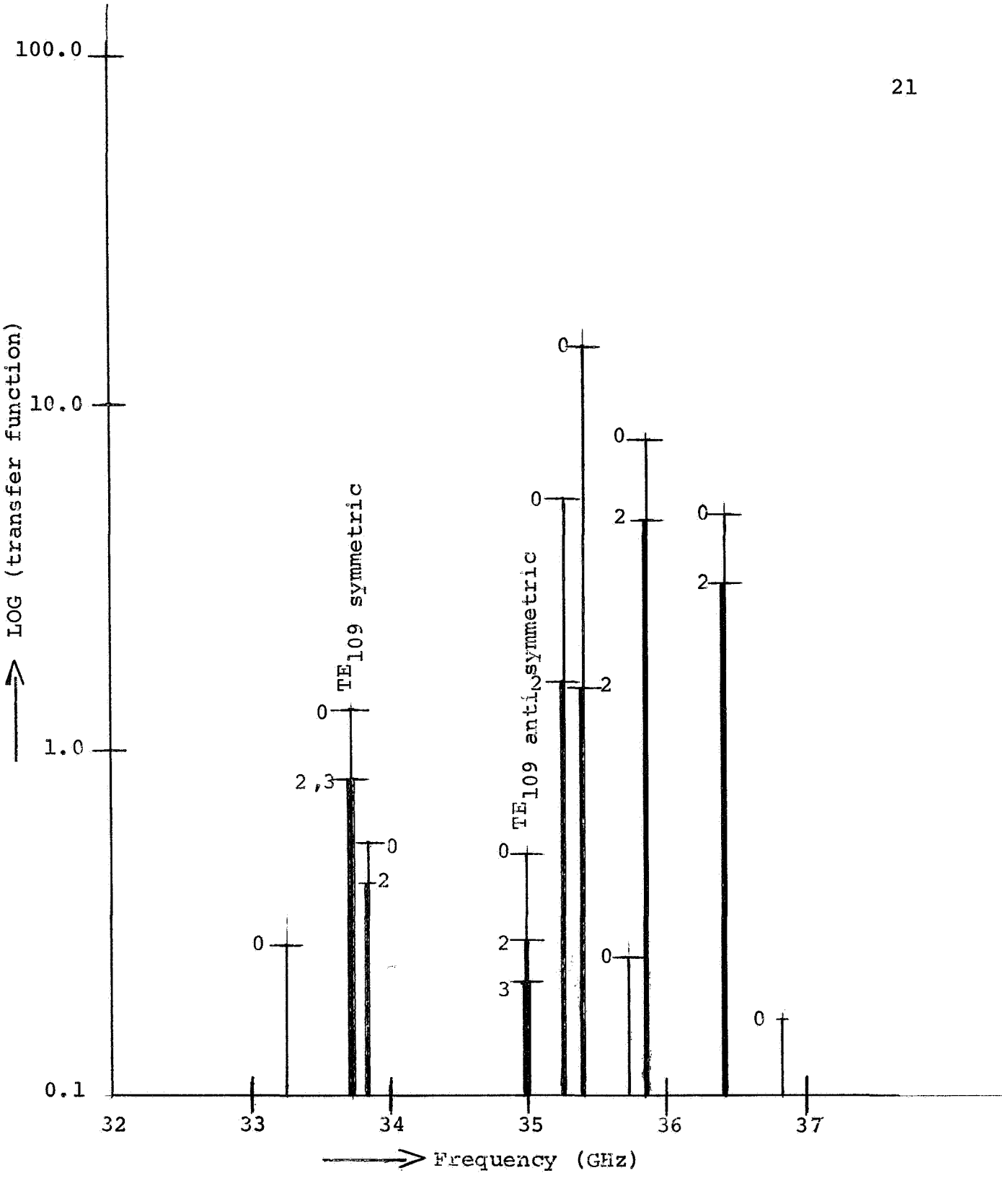

Legend: 0, magnitude, no absorbing layers
2, magnitude, AL2 inserted
3, magnitude, AL3 inserted

Fig. 6 Mode and transfer ratio spectrum for the wide-strip structure

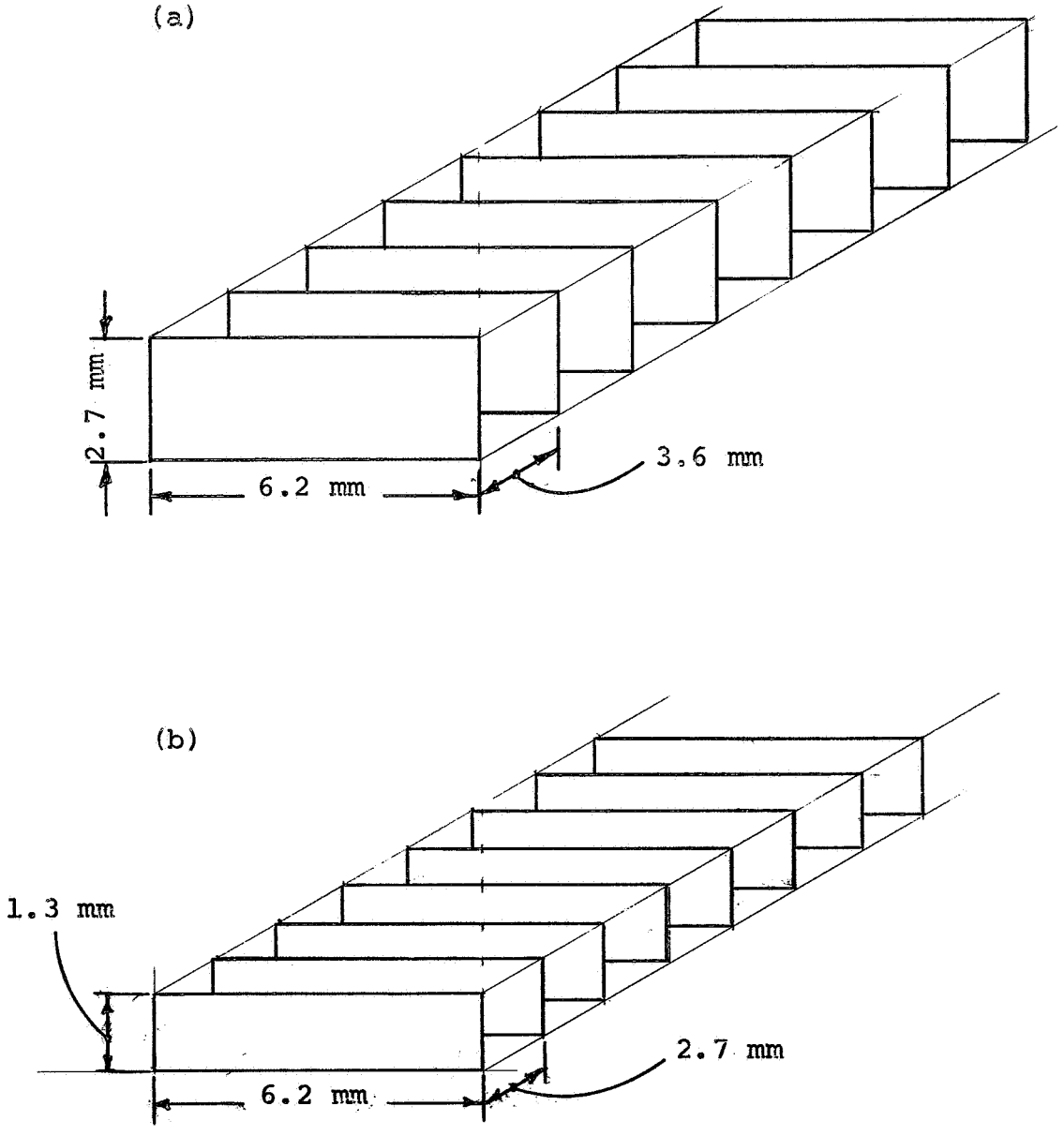

Fig. 7 Geometries of the strip structures
(a) Wide-strip structure
(b) Narrow-strip structure

The geometries of the two strip structures under investigation are illustrated in Fig. 7.

The narrow strip structure did not exhibit similar reductions of the transfer ratio. For this reason a computation of the guide wavelength and of the expected field decrease for the H-guide mode was carried out. The computation indicated that one of the observed wave modes is the TE_{109} H-guide mode which at the observed frequency is characterized by a relatively small field decrease (1/4) at the upper and lower surfaces of the cavity. Hence, if the absorbing layers are introduced, the H-guide modes are also considerably attenuated as well as the other modes with large reductions of the transfer ratios.

After identification of the wave modes by these methods, the Q-values of the major part of the wave modes were measured.

Evaluation of the measurements gives the following results:

Narrow-strip structure:

$$TE_{109} \rightarrow Q_\ell = 7174 \ (Q_u = 7289) \ @ \ f_o = 35.294 \text{ GHz}$$

$$TE_{108} \rightarrow Q_\ell = 4887 \ (Q_u = 5078) \ @ \ f_o = 34.598 \text{ GHz}$$

Wide-strip structure:

No conclusive identification of this wave mode was made.

$$TE_{109\text{antisymmetric}} \rightarrow Q_\ell = 2249 \ (Q_u = 2269) \ @ \ f_o = 35.082 \text{ GHz}$$

$$TE_{109\text{symmetric}} \rightarrow Q_\ell = 3507 \ (Q_u = 3563) \ @ \ f_o = 33.808 \text{ GHz}$$

Summarization of the results gives, for the thin-strip structure, the following data: The Q-value of the empty cavity is

Q_ℓ = 10,344 (Q_u = 10,924). Insertion of dielectric foam material for the support of the metallic strips reduces the Q to Q_ℓ = 8,331 (Q_u = 8,584). With the strips inserted, the values are Q_ℓ = 7174 (Q_u = 7289) at a frequency of about 35 GHz.

Appendix A

Determination of the Unloaded Q-Value

The unloaded Q of a resonant mode is found using methods described in a previous report (January 15, 1968). It is based on an insertion-loss measurement of the transmission-type test cavity under matched conditions. First, the cavity is replaced by a section of rectangular waveguide of the same length as the cavity including the waveguide sections on both ends. Prior to replacement, the peak of the resonance curve is displayed on the oscilloscope. The cavity is then replaced by the section of rectangular waveguide and the attenuation of a precision attenuator in series with the circuit increased until the output signal becomes equal to the level of the peak of the previously displayed resonance curve. The reading of the attenuation, in db, is then the insertion loss L [db]. It is recorded and the unloaded Q_u of the resonant cavity is found from the loaded value Q_ℓ by the following relationships,

$$Q_u = Q_\ell \left(1 + \frac{\sqrt{T}}{1 - \sqrt{T}}\right) \quad ; \quad \sqrt{T} = 10^{-L/20} \quad .$$

Appendix B

Mode Spectrum and Q-Values for Rectangular Waveguide

Various sections of rectangular waveguide were investigated to determine the resonant modes and Q-values in order to provide reference values for a comparison of the data obtained experimentally for the guiding structures for H-guides.

The measurements were carried out in the test setup described before. Copper irises were manufactured to be attached to the flanges of the waveguide sections under investigation, thereby forming a resonant cavity. A 1.95 mm hole was centered on each of the two irises to couple energy into and out of the section of waveguide.

Four sections of waveguide were tested. They are indicated by the terms TS1 to TS4 and are described as follows: TS1 and TS2 are sections of Waveline, silver-plated waveguide with lengths of 61 and 15.4 cm, respectively. TS3 has a length of 17.9 cm and is composed to two (2) sections of Waveline, silver-plated 90° twists coupled in series to provide a total of 180° of rotation of the E-plane. TS4 stands for a section of specially manufactured, heavily silver-plated waveguide that had been used to replace the copper cavity for insertion loss measurements.

The results are presented in Table 2 which shows sections of the mode spectra for the various test sections, the transfer ratios, and representative Q-values. The data can be used for the determination and comparison of the values of attenuation of the waveguide sections.

Table 2

f_o (GHz)	Transfer Ratio	Q-Value	f_o (GHz)	Transfer Ratio	Q-Value
TS1 61 cm, Waveline waveguide			TS2 15.4 cm, Waveline waveguide		
34.70	0.371	---	33.97	1.968	---
34.86	0.312	Q_ℓ=5291 Q_u=5694	34.77	2.963	Q_ℓ=5117 Q_u=6528
35.04	0.411	Q_ℓ=5892 Q_u=6289	35.58	2.368	Q_ℓ=4175 Q_u=5856
35.26	0.359	---	36.32	1.842	---
TS3 17.9 cm, Waveline 180°			TS4 20.0 cm, Special waveguide		
33.48	0.839	---	33.72	1.25	---
34.10	1.167	---	34.32	1.41	---
34.79	1.429	Q_ℓ=3552 Q_u=4342	34.90	1.61	Q_ℓ=3883 Q_u=3939
35.48	---	---	35.55	1.32	---
36.12	1.029	---	36.12	1.36	---

CHARACTERISTICS OF LOSSY-WIRE GRIDS FOR FENCE-GUIDE APPLICATIONS

Abstract

As a supplement to a preceding consideration of wire grids in which the losses of the wires were disregarded, this paper deals with their characteristics taking into account the losses. A comparison is presented of theoretical and measured values of the reflection and transmission coefficients of lossless and lossy wire grids. Wire grids made of brass and silver-plated wires are considered.

Introduction

In preceding reports, the characteristics of wire grids were considered from a viewpoint of their application as side walls in fence guides. The derived relationships are based on equations published in a few major articles.[1,2,3,4] The published equations are primarily valid for strip structures, but their use can be extended to round-wire grids by equating the strip width to twice the diameter of the grid wires. The resulting relationship taking into account the losses of the wires is

$$Zw = jZo \frac{s}{\lambda} \ln \csc \frac{\pi d}{s} + Rs \frac{s}{\pi d} (1 + j) \quad ,$$

where

Zw = wire-grid impedance,

Zo = free-space impedance,

Rs = surface resistance of the grid metal,

s = wire spacing,

d = wire diameter,

λ = free-space wavelength.

Measurements were carried out to verify the validity of this equation, particularly in the case of large wire diameters typical for the fence-guide application. Under this condition, the usually applied thin-wire approximations are no longer valid. In the previously described measurements, the losses of the wires were not taken into account and the measurement setup was not yet fully developed. Discrepancies were observed between measured and computed values of the surface impedance at that time.

Improvements were subsequently made of the measurement set-up by surrounding the wire grid more carefully with layers of absorbing material. The probe used for the field strength measurements was very carefully adjusted in a special measurement setup to give minimum coupling between its outer conductor and the actual probe section. The outer conductor has been covered by absorbing material to reduce the coupling and to eliminate waves reflected by the probe.

Two new sets of measurements were then carried out with the improved equipment. The grids were made of brass wire of 1.6 mm diameter in one set, and the wires were silver-plated in the other set of measurements. The wire losses were taken into account in these measurements.

In this report the measurements, the used relationships, and the results are described.

Measurement Setup and Measurements

The measurement setup consists of an X-band (10 GHz) klystron source connected through an isolator to a precision attenuator. Its output energy is fed through a transmission-type wave meter into a directional coupler and through a second isolator into a horn. The horn is mounted in a wooden frame and a wire grid is suspended approximately 30 cm from the mouth of the horn. Horn, wire grid, and the space behind the grid are surrounded by absorbing material to reduce undesired reflections of any kind and leakage around the wire grid. An antenna-type probe penetrates through a slot in the absorbing material into the region between the horn and the wire grid. It is attached to a traveling carriage which in turn is mounted on top of the frame. The probe facilitates measurement of the field strength distribution in front of and behind the wire grid as a function of the distance from the grid.

The standing-wave-ratio (SWR) is determined by measuring the maxima and the minima of the field strength. The transmission coefficient is found by measuring additionally the field strength behind the wire grid. The SWR has a maximum measurable value since spurious indications in the minimum of the field strength in front of the grid are preventing accurate determinations of the minimum's value. The threshold for the measurement of small values of field strength is about 30 db below the maximum. The measurements are made by adjusting the attenuator in the input waveguide of the horn to give constant

indications of the probe output. The output voltage of the probe is rectified by a detector and fed into an amplifier-indicator typical for SWR measurements.

The wire grids under investigation have a size of about 30 x 30 cm. Four grids are made of 1.6 mm diameter brass wire spaced at 4.0, 8.0, 12.0, and 16.0 mm. The wires can be replaced by silver-plated wires with the same spacing.

The measurements are carried out by moving the probe from the grid toward the horn and by determining the maxima and minima of the field strength. Two series of measurements are carried out, one with the probe moving exactly in front of a grid wire and the other with the probe moving in a plane between the wires. The measurements are repeated and the results averaged. Subsequently, the probe is carefully transferred behind the grid and the field distribution determined in this region. Basically, it is constant; small residual variations, however, are observed which are the results of spurious waves. The effects of these waves can be practically eliminated by averaging the measured values of field strength.

Major Relationships

The reflection and transmission coefficients are, using notations suitable for computer programming, given by

$$R = \frac{Er}{Ei} \quad , \tag{1}$$

$$T = \frac{Et}{Ei} \quad , \tag{2}$$

where

Er is the reflected wave,

Et is the transmitted wave,

Ei is the incident wave.

The propagation of plane waves through the wire grid can be considered by an analogous wave propagation along a transmission line. The wire grid is represented by a shunt admittance, 1/Zw coupled parallel to the line with a characteristic impedance Zo. The coupling in parallel of the impedances gives

$$Z = \frac{Zw \cdot Zo}{Zw + Zo} \quad . \tag{3}$$

The reflection coefficient becomes

$$R = \frac{Z - Zo}{Z + Zo} = - \frac{1}{1 + 2\ Zw/Zo} \quad . \tag{4}$$

The transmission coefficient is

$$T = 1 + R = \frac{2\ Zw/Zo}{1 + 2\ Zw/Zo} \quad . \tag{5}$$

The grid impedance is given by

$$Zw/Zo = \left(\frac{Rs}{Zo} \cdot \frac{s}{\pi D}\right) + j \cdot \left\{\frac{Rs}{Zo} \cdot \frac{s}{\pi D} + \frac{s}{\lambda} \cdot \left[\ln\left(\csc \frac{\pi D}{s}\right) + F\right]\right\} \quad , \tag{6}$$

where F is a correction term introduced by MacFarlane[1]. A loss factor can be introduced which takes into account the losses of the wire grids in terms of the field strength of the incident wave,

$$E\ell = (1 - |R|^2 - |T|^2)^{1/2} \quad . \tag{7}$$

Two computer programs were developed, one for the determination of the theoretical values of the interesting quantities, namely, $|R|$, $|T|$, SWR, and $E\ell$, and one for the evaluation of the measured data. The values of Rs used were $2.54 \times 10^{-7} \sqrt{\text{freq.}}$ for silver and $5.14 \times 10^{-7} \sqrt{\text{freq.}}$ for brass.

Computer Programs and Results

The flow chart of the computer program for the determination of the theoretical values of the observables is shown on the following pages together with an explanation of flow-chart symbols. The following Table 1 contains the results. The results of the experiments which were evaluated by the second computer program are shown on Table 2.

The results indicate that the effects of the wire losses are relatively small if the grids are made of thick wires. The effects become more pronounced at small separation of the wires.

Explanation of Flow Chart Symbols

The equations designated by number can be found in the preceding text.

XLAM = the wavelength

D = the wire diameter

S = the center-to-center wire spacing

F = the MacFarlane correction factor

R = an input variable to calculate wire surface resistivity

A = an input variable to supply the print-out label

RS = the wire surface resistivity as calculated by

$$RS = R \cdot \left[\frac{3 \times 10^{11}}{XLAM}\right]^{1/2}$$

RIP = the surface resistance of the grid referenced to ZO

XIP = the surface reactance of the grid referenced to ZO

XGP = the MacFarlane reactance of the grid referenced to ZO

XTP = the total reactance of the grid

XTP = XIP + XGP

RHOMG = the magnitude of the reflection coefficient

TAUMG = the magnitude of the transmission coefficient

SWR = the voltage standing wave ratio as culated from the reflection coefficient

SWRDB = the SWR expressed in decibels

EL = the loss factor

Flow Chart of Theoretical Program

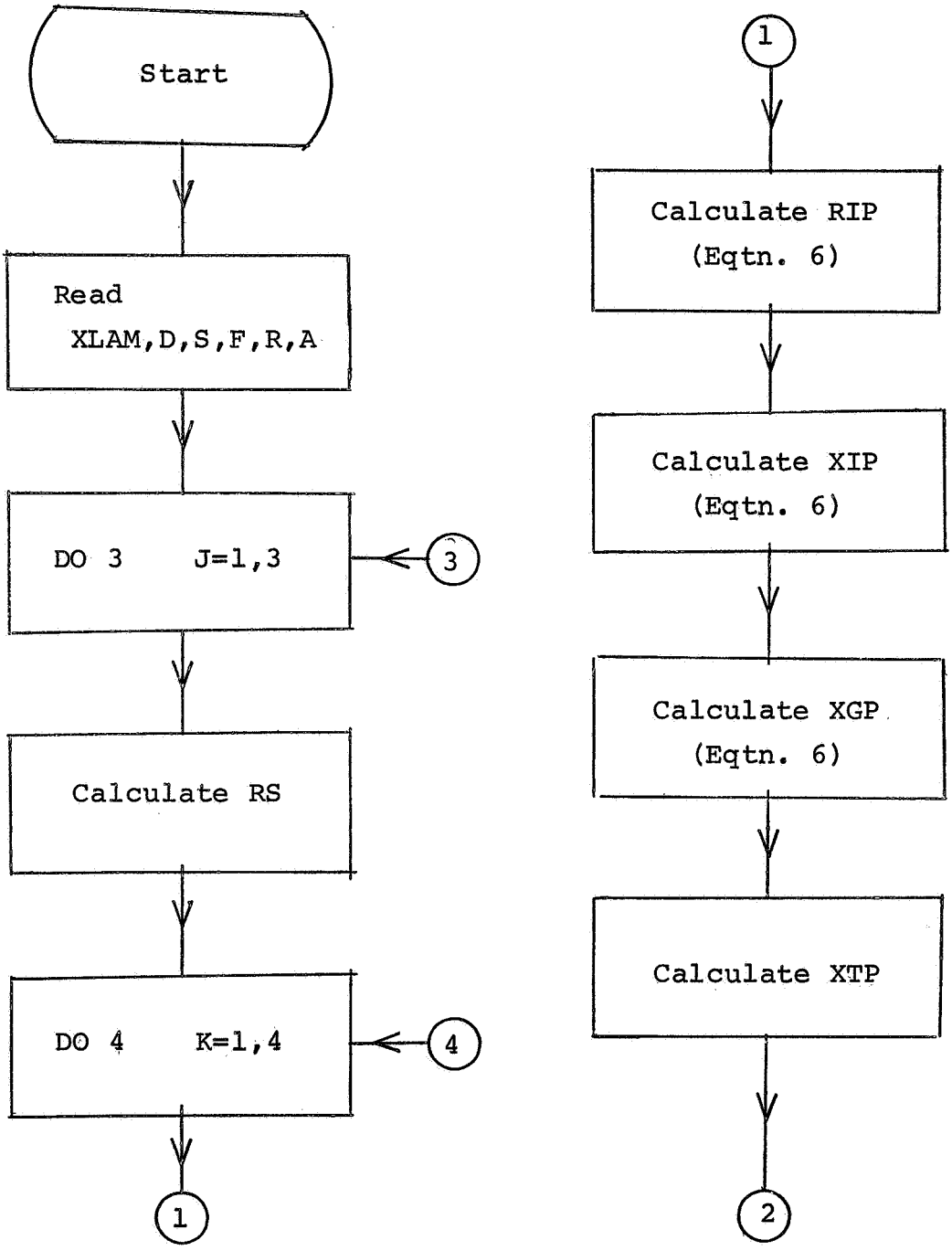

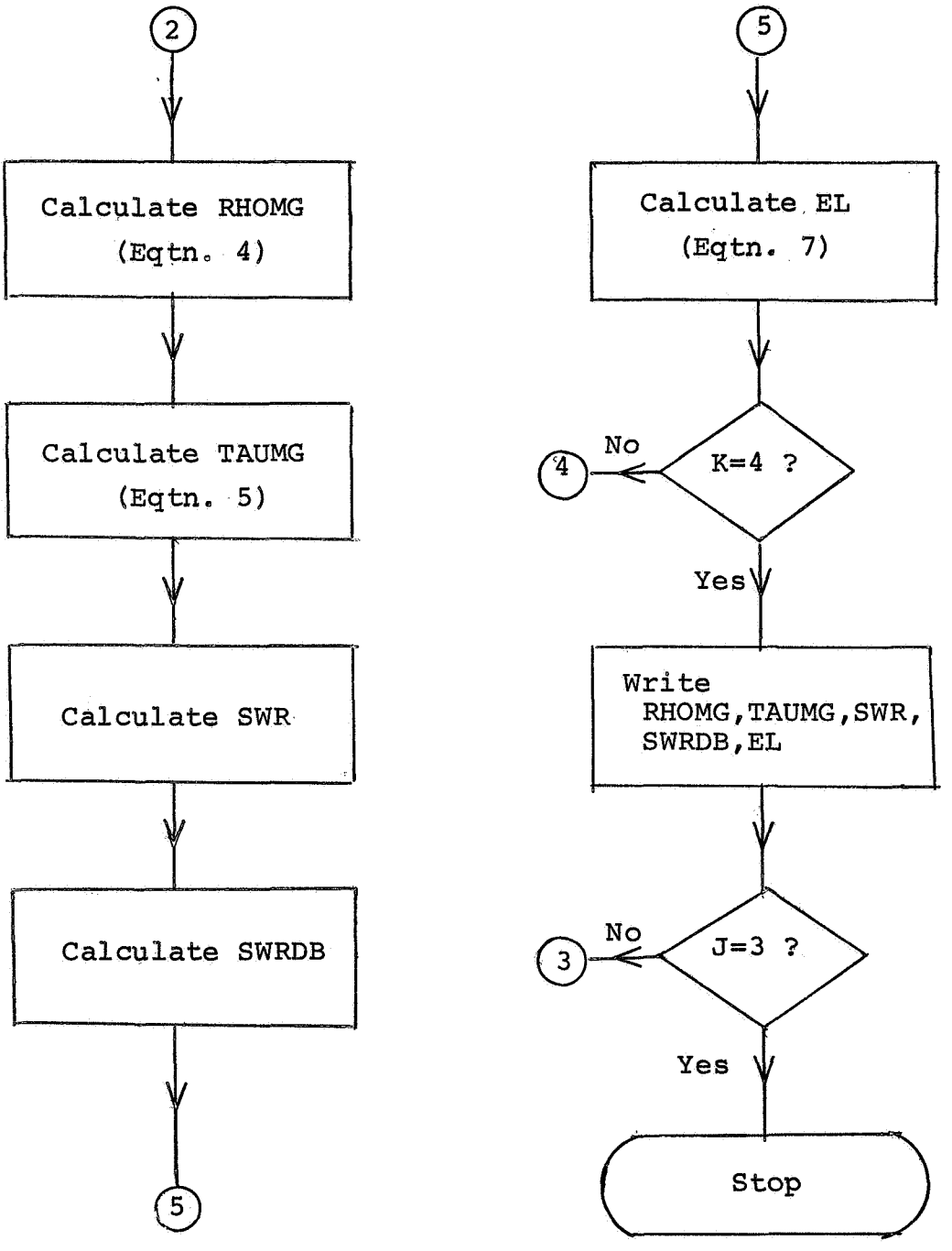
2
Calculate RHOMG
(Eqtn. 4)
Calculate TAUMG
(Eqtn. 5)
Calculate SWR
Calculate SWRDB
5
5
Calculate EL
(Eqtn. 7)
No
4
K=4 ?
Yes
Write
RHOMG,TAUMG,SWR,
SWRDB,EL
No
3
J=3 ?
Yes
Stop

Table 1

Theoretical data for lossless wire, silver wire, and brass wire.

Lossless wire

S	RHOMG	TAUMG	SWRDB	LOSS
4.0	0.99987	0.01590	83.386	0.0
8.0	0.95813	0.28634	33.396	0.0
12.0	0.79940	0.60080	19.055	0.0
16.0	0.60394	0.79603	12.148	0.0

Silver wire

S	RHOMG	TAUMG	SWRDB	LOSS
4.0	0.99977	0.01610	78.301	0.01464
8.0	0.95788	0.28648	33.345	0.01838
12.0	0.79911	0.60084	19.042	0.02027
16.0	0.60372	0.79700	12.142	0.01768

Brass wire

S	RHOMG	TAUMG	SWRDB	LOSS
4.0	0.99965	0.01612	75.022	0.02083
8.0	0.95763	0.28661	33.292	0.02821
12.0	0.79882	0.60088	19.028	0.02882
16.0	0.60350	0.79697	12.136	0.02515

Table 2

Experimental data for silver-plated wire and brass wire.

Silver-plated wire

S	RHOMG	TAUMG	SWRDB	LOSS
4.0	0.99927	0.03518	67.678	0.01461
8.0	0.97121	0.23737	36.680	0.02010
12.0	0.74156	0.67063	16.568	0.01880
16.0	0.65545	0.75499	13.631	0.01919

Brass wire

S	RHOMG	TAUMG	SWRDB	LOSS
4.0	0.99904	0.03257	65.477	0.02943
8.0	0.95023	0.31028	31.845	0.02799
12.0	0.77345	0.63324	17.869	0.02791
16.0	0.54484	0.83823	10.612	0.02270

References

1. G. G. MacFarlane, Surface Impedance of an Infinite Parallel-Wire Grid at Oblique Angles of Incidence, J. Inst. Elec. Engrs., pt3A, vol. 93, p1523-1527; 1946

2. N. Marcuvitz, Waveguide Handbook, p280-284, M. I. T. Radiation Laboratory Series 10, McGraw-Hill, New York

3. J. R. Wait, Effective Impedance of a Wire Grid Parallel to the Earth Surface, IRE Trans. on Ant. and Prop., vol. AP-10, p538-542, September 1962

4. E. A. Lewis and J. Casey, Electromagnetic Reflection and Transmission by Gratings of Resistive Wires, J. Appl. Phys., vol. 23, p605-608; June, 1952

A NEW CONCEPT IN FENCE-GUIDE DESIGN

The fence guide is an H-guide with the solid side walls replaced by wire grids. The structure is illustrated in Fig. 1. The possibility to design millimeter wave circuitry in the form of a sheet of dielectric material with the path of the electromagnetic waves confined between the wire grids offers a way of simplified production of circuitry in comparison with designs based on rectangular waveguides. Simple production seems possible by placing wires in an appropriate holder, then forming the dielectric sheet by customary fabrication processes, and then removing the wire holder.

Preliminary measurement of the characteristics of a fence-guide model indicated some difficulties primarily in the form of high attenuation which had to be overcome before a competitive structure can be designed. As a first step, a program was initiated for developing relationships for the description and analysis of wire grids for fence-guide design. Measurements were carried out to verify the validity of the derived equations. It was found that a modification of the familiar equations for the surface impedance of thin-wire grids led to relationships which are also valid for grids with thick wires typical for the fence guide. Recent results of measurements of the characteristics of thick wire grids are presented in this report. The relationships can now be used for the determination of optimized parameters of an advanced prototype fence guide.

One of the unfavorable characteristics observed in the study of the preliminary fence-guide model was the rather high attenuation. This can be attributed in part to the preliminary design, in which rather thin wires were used for the grid. By the use of thick wires, a considerable reduction of the losses can be obtained. Radiation and leakage of power through the wire grids, however, is always present in the case of the customary design. A new design concept is being formulated at present to reduce the radiation losses to a minimum. Derivation of the relationships presented on pages 12 to 14 of the preceding Progress Report[1] led to this concept.

The relationship from which the new concept evolved is that which describes the surface impedance of wire grids, Z_s used as the side walls of the fence guide [Eq. (21)]. The impedance is given by

$$Z_s = \frac{Zw}{1 + (Zw/Zo)\cos\theta} \quad , \tag{1}$$

where Z_w is the shunt impedance of the lossy wire grid, defined on page 32 of this report, Z_o is the free-space impedance and $\cos\theta$ is related to the guide wavelength of the fence guide by

$$\cos\theta = \sqrt{1 - (k_z/k_o)^2} \quad . \tag{2}$$

The angle θ is the angle against the normal to the grid surface under which the waves leaking through the grid are radiated into the outer region. The constant k_z is the propagation constant within the guide in longitudinal direction and k_o is the corresponding constant outside in the direction of the propagating waves.

Since it is desirable to make the surface impedance of the side walls as small as possible, this goal can be achieved by reducing the shunt impedance of the wire grid Z_w and by reducing cos θ. Increase of the wire diameter and decrease of spacing between the wires accomplishes the former reduction. The reduction of cos θ, which in the center of the transmission band of waveguides has a value of about 0.75, can be obtained by reducing the propagation constant, k_z. Measures for reducing this quantity will thus also reduce Z_s and the losses in the guide. For $k_z = k_o$, cos θ becomes 0 and no radiation occurs. If k_z is larger than k_o, so-called "invisible radiation" occurs and the field distribution has the form of non-radiating surface waves. The new concept of fence-guide design is based on attempts to lower the guide losses by reducing the propagation constant, k_z.

The following measures can be used for the reduction of k_z:

1. Increase of the guide width above the value of standard waveguides.
2. Application of dielectric loading within the guide.
3. Reduction of the dielectric-slab thickness outside the guide.

An increase of width of the guide is permissible. However, it is limited by the possibility of generation of higher-order modes in the case of discontinuities and in components.

The application of dielectric loading of the fence guide seems to be at present the most promising method of radiation

reduction. Several approaches are possible for such loading. Three examples are shown in Fig. 2. Figure 1a illustrates the method of having the thickness of the dielectric slab increased within the guide. This can be combined with method No. 3 of the above list. Introduction of ridges of the dielectric slab in the center of the guide is shown in Fig. 2c. This method may have additional advantages by creating a field distribution within the guide which additionally may reduce radiation through the grid. Lamination of the slab in the fence guide with reduced thickness outside the guide or addition of slabs within the guide represents a third example which also may be combined with method No. 3 of the above list.

It seems thus that the proposed concept of fence-guide design promises to reduce the losses of this guide to approach values typical for H-guides with solid walls, where Z_s is represented by the intrinsic surface impedance of the material of the solid walls. Further numerical considerations of the proposed structures will be necessary before the principle can be applied for the design of an optimized guide.

References

1. Progress Report on Study of Rectangular-Guide-Like Structures for Millimeter Wave Transmission. Grant NGR 34-002-047/S1, October 15, 1968

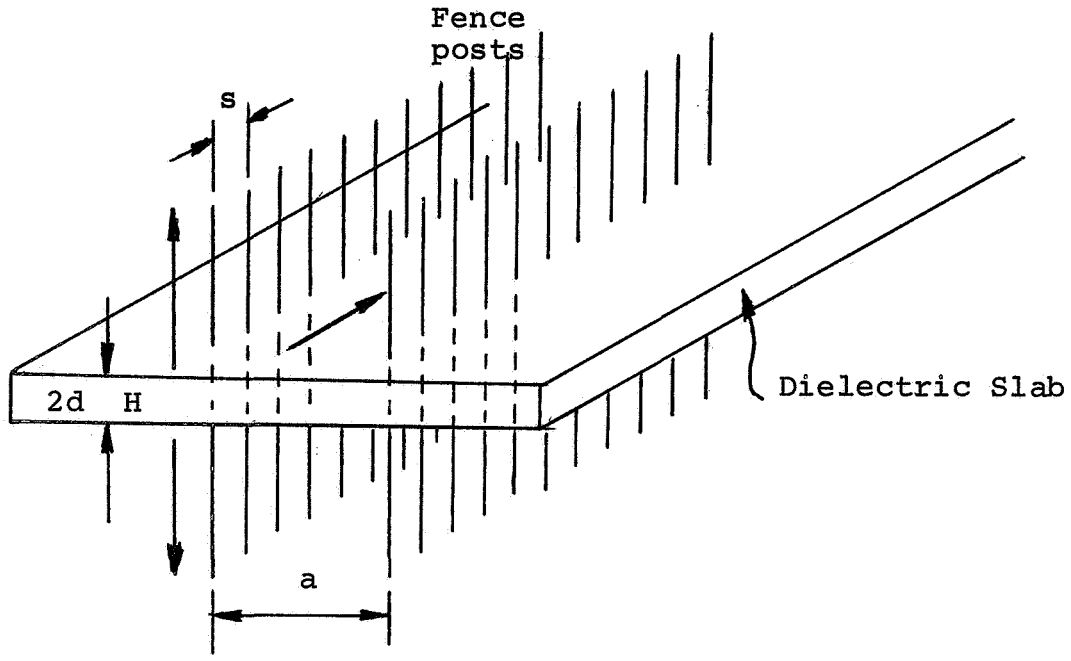

Fig. 1 Conventional fence guide

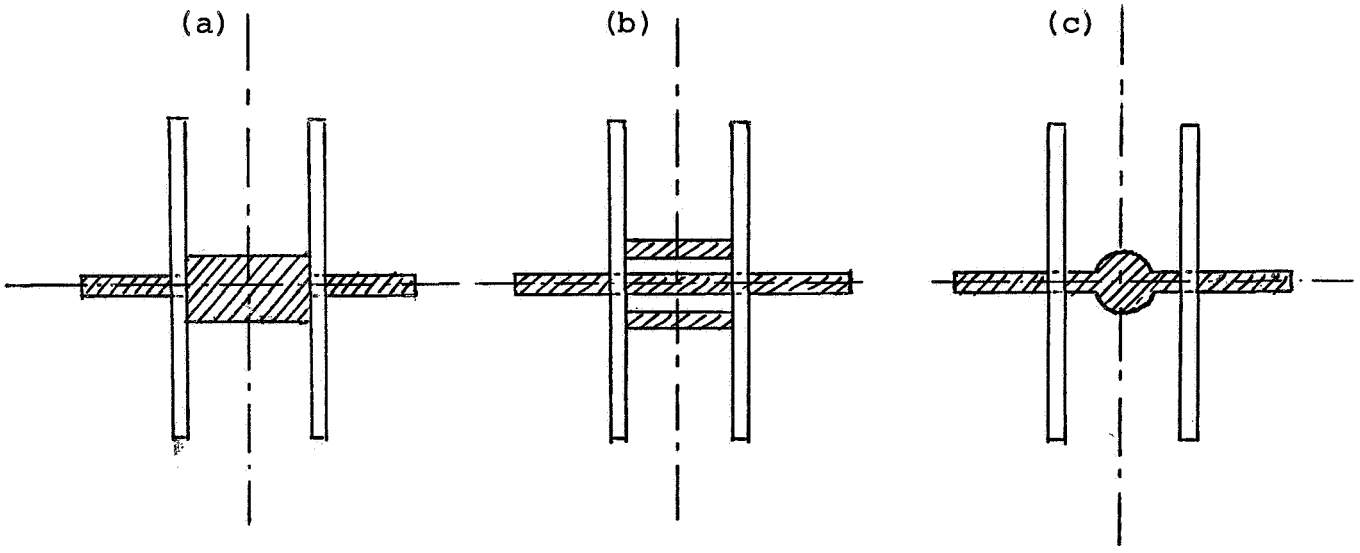

Fig. 2 Low-leakage fence-guide cross sections

(a) Increased internal slab thickness
(b) Multiple-slab guide
(c) Centrally dielectric-loaded guide

H-GUIDE WAVELENGTH AND ATTENUATION

Abstract

Previously derived equations for the attenuation constants and guide wavelength of a dielectric H-guide were modified and normalized to obtain more general and in part frequency independent relationships. The results are given in terms of the dielectric slab thickness and plate separation expressed as fractions of the wavelength, of the medium properties of the dielectric slab given by ε_r, and of the wall conductivity represented by the surface resistance R_s. Graphs are presented showing normalized guide wavelength, total attenuation, wall attenuation, and dielectric attenuation as a function of dielectric slab thickness with plate separation as a parameter.

Introduction

The presented equations are based on relationships derived at the beginning of the grant period published in part in previous reports [1].

Previous work gave curves of the attenuation constant as a function of the relative permittivity for the H-guide at 10.0 GHz with the normalized exponential decay constant, p, as a parameter. A more useful set of curves might be a plot of attenuation constant vs. dielectric thickness for a particular dielectric constant. Necessary calculations to obtain such curves also yield the guide wavelength so that curves of the guide wavelength vs. dielectric slab thickness may also be plotted.

A general solution independant of frequency would be convenient. However, the attenuation curves are necessarily functions of frequency and such solutions are not possible. In the case of guide wavelength, this approach can be used, by normalizing the dimensions and the guide wavelength with respect to free space wavelength. The development which follows is formulated in this manner.

Derivations of the Equations

The following equations are needed. (Equation numbers are taken from the reference.)

$$k_x^2 + k_y^2 + k_z^2 = \varepsilon_r k_o^2 \tag{5.14}$$

$$k_y = \pi/b \tag{5.15}$$

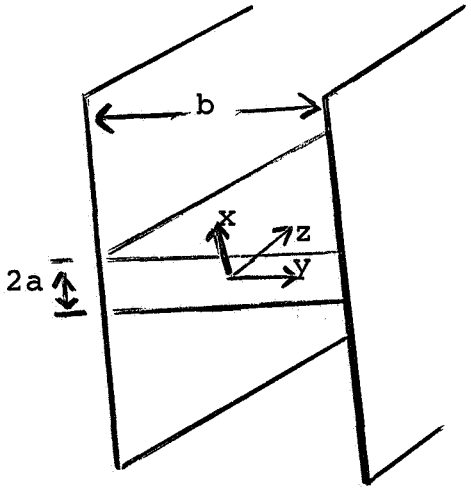

Fig. 1 H-guide dimensions and coordinate system

$$k_o^2 = \omega^2 \mu_o \varepsilon_o \tag{5.16}$$

$$k_o^2 = -\alpha_x^2 + k_y^2 + k_z^2 \tag{5.29}$$

$$\varepsilon_r \alpha_x = k_x \tan (k_x a) \tag{5.38}$$

$$h^2 = k_x^2 + \varepsilon_r^2 \alpha_x^2 \tag{5.47}$$

$$p = \alpha_x / k_o \tag{5.77}$$

$$q = k_y / k_o \tag{5.78}$$

$$H = ah^2 / k_o \tag{5.84}$$

$$\alpha_d = \frac{\tan(\delta)\, k_o}{2} \cdot \frac{\varepsilon_r p \,[H + p\,(2-\varepsilon_r + 2p^2)]}{\sqrt{1 + p^2 - q^2}\,[Hp + \varepsilon_r(\varepsilon_r - 1)]} \tag{5.85}$$

$$\alpha_b = \frac{2R_s \varepsilon_r}{b\sqrt{\frac{\mu_o}{\varepsilon_o}}} \cdot \frac{q^2 p \,[H + \varepsilon_r p]}{\sqrt{1 + p^2 - q^2}\,(1 + p^2)\,[Hp + \varepsilon_r(\varepsilon_r - 1)]} \tag{5.88}$$

$$\alpha_a = \frac{2R_s \varepsilon_r}{b\sqrt{\frac{\mu_o}{\varepsilon_o}}} \cdot \frac{q^2\,(\varepsilon_r - 1 - p^2}{\sqrt{1 + p^2 - q^2}\,(1 + p^2)\,[Hp + \varepsilon_r(\varepsilon_r - 1)]} \tag{5.90}$$

The definition of the coordinate system and dimensions is given in Fig. 1. The other variables are defined as follows.

k_x, k_y, k_z = separation constants for the wave equation in the dielectric region ($|x| < a$).

k_o = free space wave number = $\omega \sqrt{\mu_o \varepsilon_o}$

ε_r = relative dielectric constant of slab

α_x = exponential decay constant in air region (separation constant, $|x| > a$). Fields vary with x in this region as exp $[-\alpha_x x]$

p = normalized decay constant

q = normalized y-direction separation constant

tan (δ) = loss tangent of dielectric

R_s = surface resistivity of the metallic walls

α_d = attenuation constant due to losses in dielectric

α_b = attenuation constant due to losses in walls in dielectric region

α_a = attenuation constant due to losses in walls in air region.

Defining two new parameters,

$$r = k_x/k_o \tag{1}$$

and

$$s = k_z/k_o = \lambda_o/\lambda_g \tag{2}$$

we simplify (5.14) to

$$r^2 + q^2 + s^2 = \varepsilon_r \tag{3}$$

and (5.29) to

$$-p^2 + q^2 + s^2 = 1. \tag{4}$$

combining (3) and (4) yields

$$1 + p^2 = \varepsilon_r - r^2 \quad , \tag{5}$$

and (5.38) becomes

$$\varepsilon_r \, p = r \tan (k_o \, r \, a) \quad . \tag{6}$$

Hence, (5) and (6) yield

$$p^2 = \frac{r^2 \tan^2 (k_o ra)}{\varepsilon_r^2} = \varepsilon_r - 1 - r^2 \tag{7}$$

or

$$r^2 \left[1 + \frac{\tan^2 (k_o ra)}{\varepsilon_r^2} \right] = \varepsilon_r - 1 \tag{8}$$

Normalizing the dimensions with respect to the free space wavelength, we define

$$a' = 2a/\lambda \tag{9}$$

and

$$b' = b/\lambda \tag{10}$$

thus

$$k_o ra = \frac{2\pi}{\lambda} \cdot r \cdot a = \pi a' r \tag{11}$$

and

$$q = \frac{k_y}{k_o} = \frac{\pi/b}{k_o} = \frac{\pi}{b.\frac{2\pi}{\lambda}} = \frac{1}{2b'} \tag{12}$$

Also, (5.16) implies

$$k_o = \omega\sqrt{\mu_o \varepsilon_o} = \frac{\omega}{c} = \frac{2\pi f}{c} \tag{13}$$

and hence

$$h^2 = k_o^2 \ (r^2 + \varepsilon_r^2 \ p^2) \quad . \tag{14}$$

Thus,

$$H = ak_o \ (r^2 + \varepsilon_r^2 \ p^2)$$

$$= \pi a' \ (r^2 + \varepsilon_r^2 \ p^2) \tag{15}$$

We note also from (4) that

$$s^2 = 1 + p^2 - q^2 \quad . \tag{16}$$

Summarized Calculation Procedure

From this development, we can summarize a procedure for determining the normalized guide wavelength (λ_g / λ_o), and the attenuation constant for a given configuration and frequency. We assume that a, b, λ, ε_r, R_{so}, and tan (δ) are known, where

$$R_s = R_{so} \times 10^{-7} \sqrt{f} \ ,$$

the surface resistivity of the walls at the frequency f. Then we proceed with

$$q = \frac{1}{2b'} \quad , \tag{12}$$

and

$$p = \sqrt{\varepsilon_r - 1 - r^2} \tag{7}$$

Then we solve the transcendental equation

$$r^2 \left[1 + \frac{\tan^2(\pi a' r)}{\varepsilon_r^2} \right] = \varepsilon_r - 1 \tag{17}$$

for the parameter r. This allows the computation of λ_g / λ from

$$s = \frac{\lambda_g}{\lambda} = \sqrt{\varepsilon_r - q^2 - r^2} \tag{3}$$

or from

$$s = \sqrt{1 + p^2 - q^2} \quad . \tag{4}$$

Since

$$k_o = 2\pi f \; / \; 3 \times 10^8 \quad , \tag{13}$$

and

$$\sqrt{\frac{\mu_o}{\varepsilon_o}} = 120\pi \quad , \tag{18}$$

and

$$b = b' \cdot \lambda = b' \cdot \frac{3 \times 10^8}{f} \quad , \tag{19}$$

we have

$$\frac{R_s}{b\sqrt{\frac{\mu_o}{\varepsilon_o}}} = \frac{R_{so} \times 10^{-7} \sqrt{f}}{b' \times \frac{3 \times 10^8}{f} \cdot 120\pi} \tag{20}$$

or

$$\frac{R_s}{b\sqrt{\frac{\mu_o}{\varepsilon_o}}} = \frac{R_{so}}{b'} f^{3/2} \times \frac{10^{-15}}{360\pi} \tag{21}$$

We can then rewrite (5.85), (5.88), (5.90) as

$$\alpha_d = \frac{\tan(\delta).\pi.f.}{3 \times 10^8} \quad \frac{\varepsilon_r p\,[H + p\,(2 - \varepsilon_r + 2p^2)]}{s\,[Hp + \varepsilon_r\,(\varepsilon_r - 1)]} \tag{22}$$

$$\alpha_b = \frac{R_{so} f^{3/2} \times 10^{-15}}{180\pi\, b'} \quad \frac{\varepsilon_r\, q^2\, p\,[H + \varepsilon_r p]}{s(1 + p^2)\,[Hp + \varepsilon_r(\varepsilon_r - 1)]} \tag{23}$$

$$\alpha_a = \frac{R_{so} f^{3/2} \times 10^{-15}}{180\,\pi b'} \quad \frac{\varepsilon_r\, q^2\,(\varepsilon_r - 1 - p^2)}{s(1 + p^2)\,[Hp + \varepsilon_r(\varepsilon_r - 1)]}\,. \tag{24}$$

Computed Results

Curves for total attenuation constant

$$\alpha = \alpha_a + \alpha_b + \alpha_d \tag{25}$$

as a function of dielectric slab thickness with plate separation as a parameter were obtained using a digital computer and a plotter. Similarly, curves of normalized guide wavelength for the same guides. Plate separations varied from 0.55λ to 2.3λ and dielectric slab thickness varied from 0.0λ to 0.975λ. Thus, the range of values for p is from 0 to 0.5 for Eccofoam ($\varepsilon_r = 1.4$, $\tan(\delta) = 4 \times 10^{-3}$), from 0 to 1.1 for Rexolite ($\varepsilon_r = 2.53$, $\tan(\delta) = 6.6 \times 10^{-4}$), and from 0 to 2.2 for a hypothetical dielectric ($\varepsilon_r = 6.0$, $\tan(\delta) = 5 \times 10^{-4}$). Hence, with an H-guide

of total height 2 λ, at the maximum thickness of the dielectric (p is independent of plate separation) the decay of the fields can be determined as follows. Since

$$p = \frac{\alpha_x}{k_o} \tag{5.77}$$

and since α_x is in nepers per meter and k_o is in radians per meter, then p represents the decay of the field in nepers per radian. Since there are 2π radians in one wavelength, the total decay in nepers can be obtained by multiplying p by 2π times the number of wavelengths in the height (from the dielectric to the edge of the plate s) in wavelengths. Thus, for a total height of 2 λ, we have total decay in nepers for Eccofoam as 3.14, for Rexolite as 6.9, and for the hypothetical dielectric as 13.8. To obtain the decay, we raise the Napierian base e to the negative of these figures so that for Eccofoam we have a decay of .043, for Rexolite .001, and for the dielectric the ratio is essentially zero.

The curves showing the normalized guide wavelength and the attenuation constants vs. a' are given in Figures 2 and 3, respectively. In addition, separate curves of wall losses and dielectric losses are given.

References

1. Bostian, Ch., Tischer, F. J., and Propst, R. H., in: A Study of H-Guides with Artificial Dielectrics. Progress Report, Grant NGR-34-002-047/S1, January 15, 1968, National Aeronautics and Space Administration, Washington, D. C.

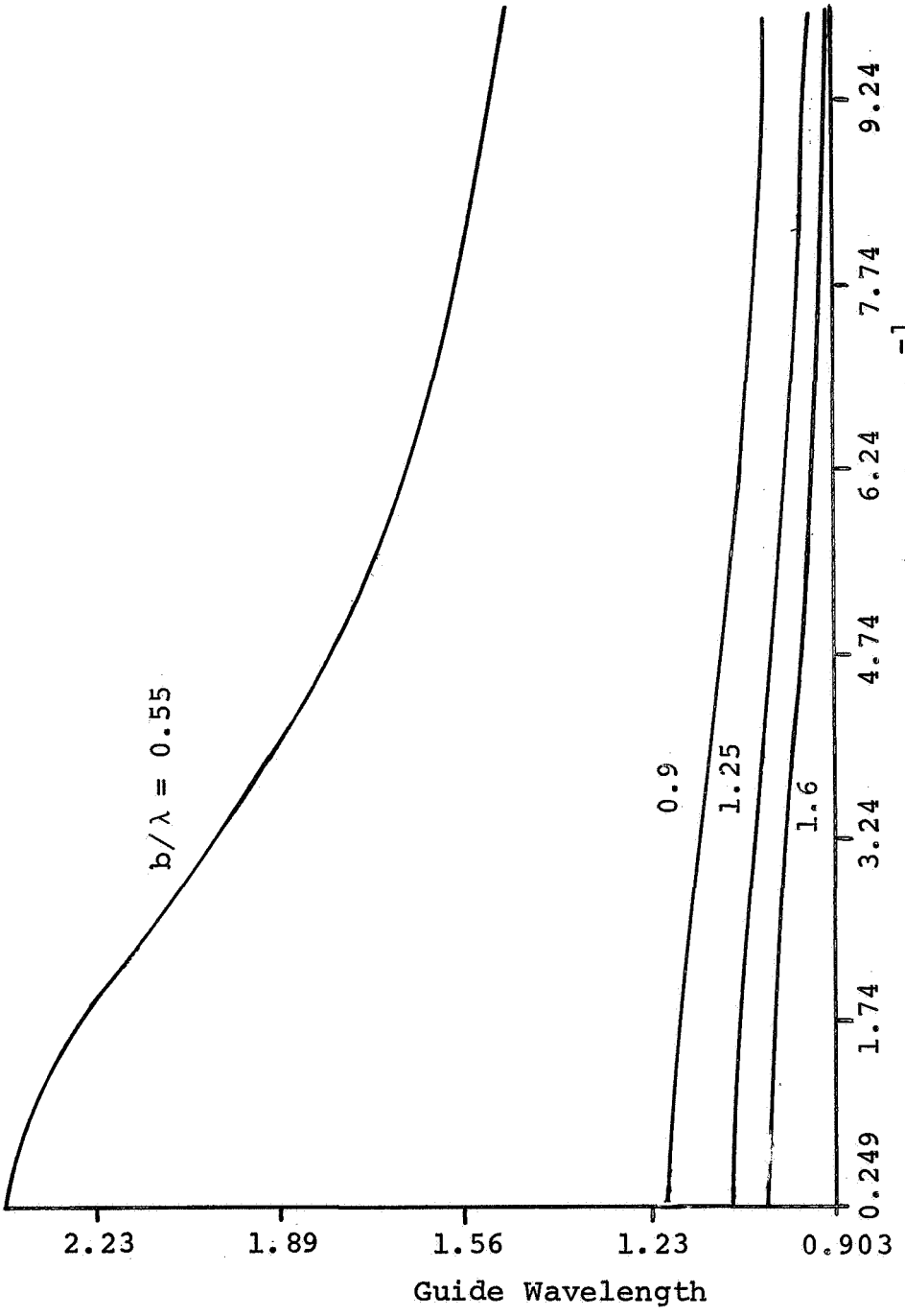

Fig. 2 Guide wavelength versus normalized thickness of the dielectric slab for Eccofoam

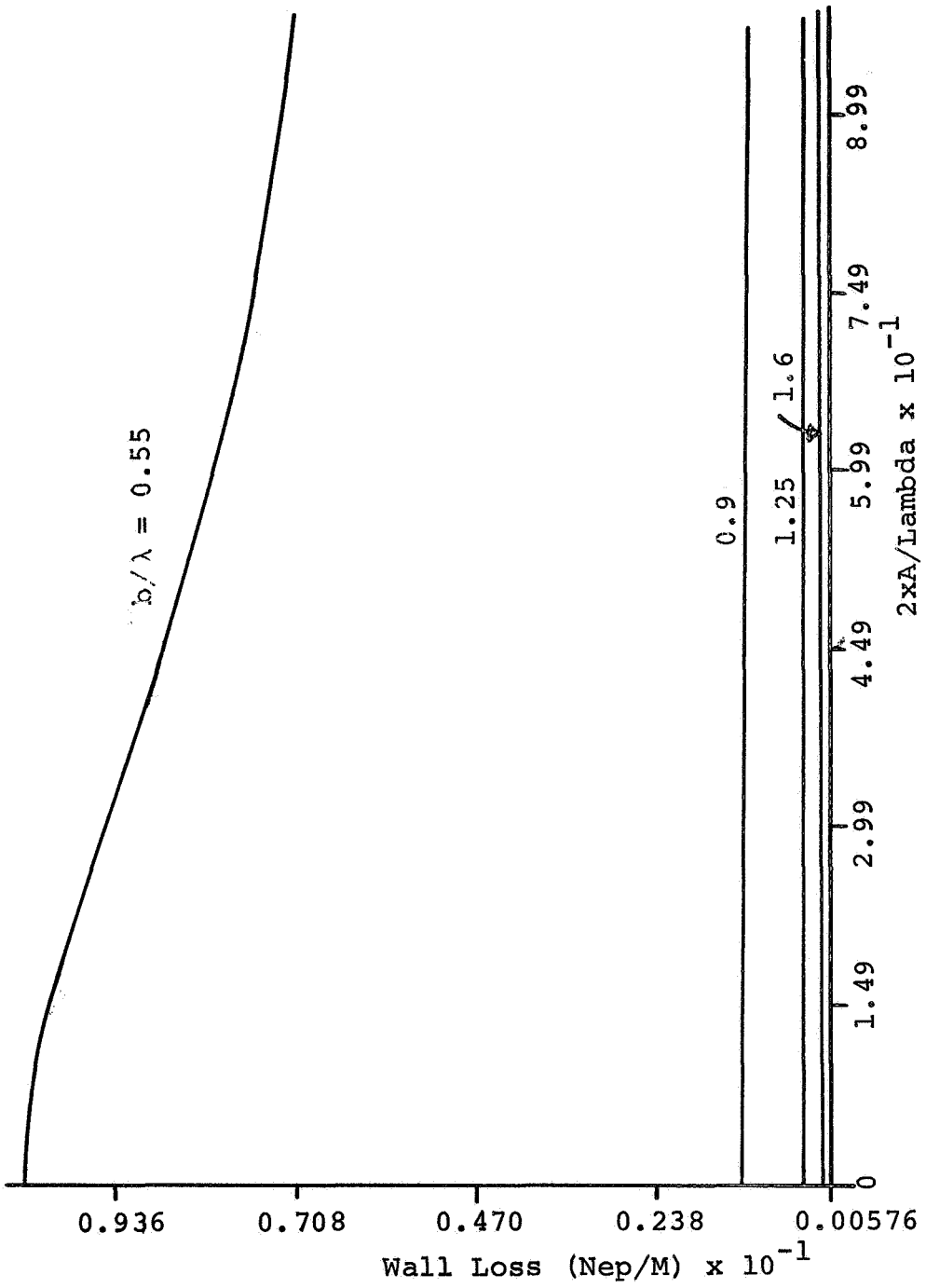

Fig. 3 Attenuation due to wall losses as a function of dielectric-slab thickness (b = guide width) for Eccofoam

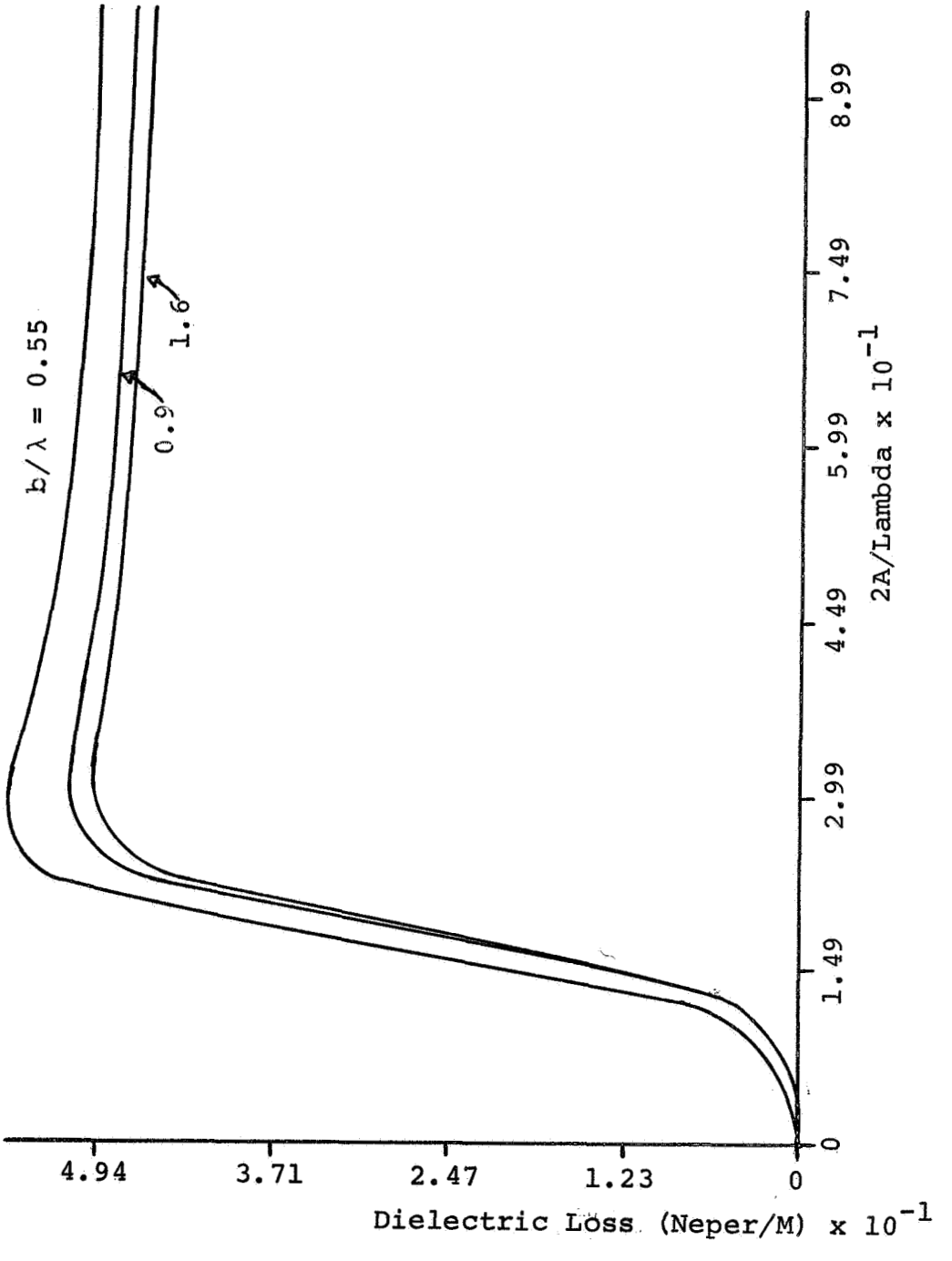

Fig. 4 Attenuation due to dielectric losses for Eccofoam

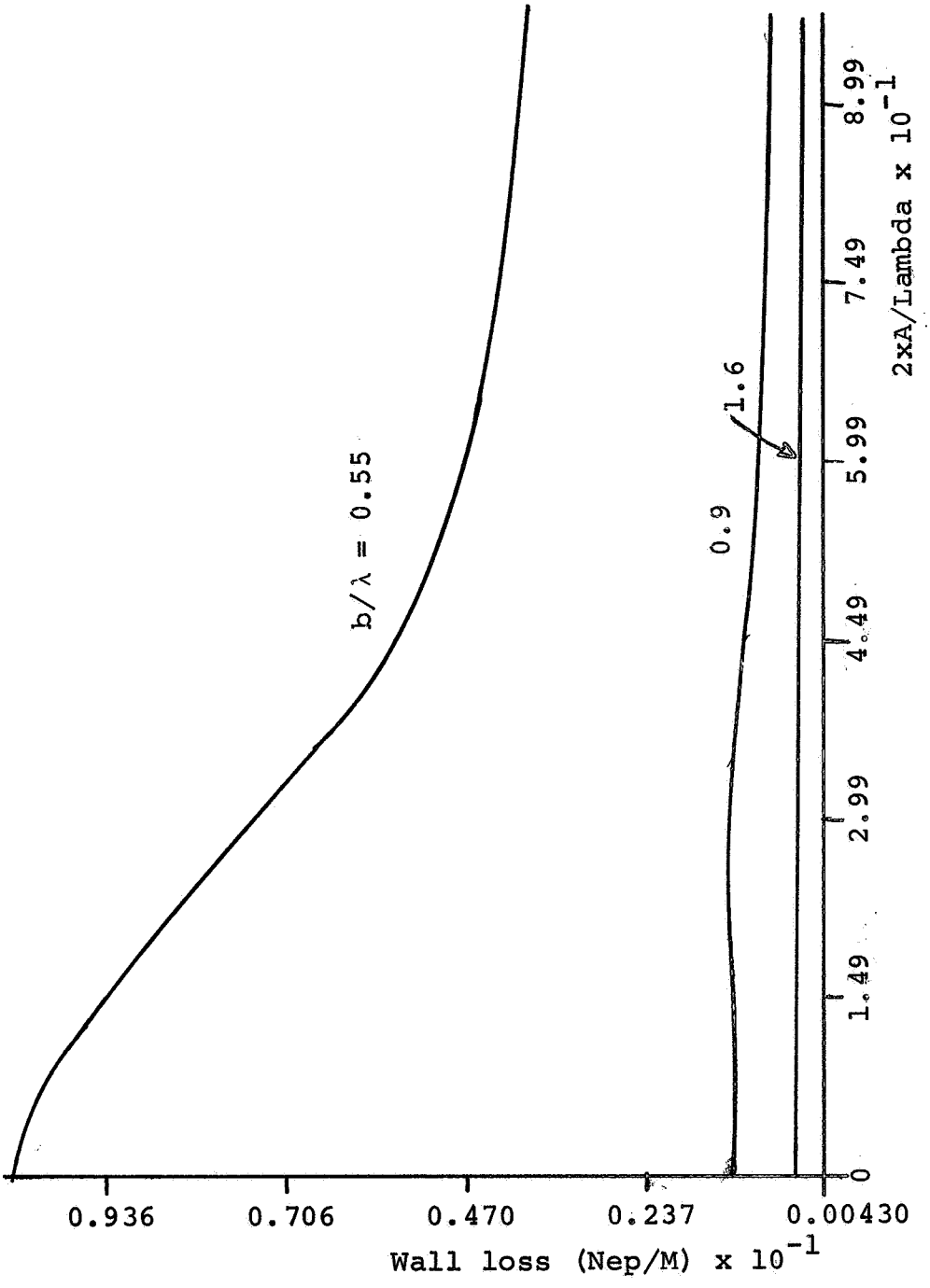

Fig. 5 Attenuation due to wall losses for Rexolite

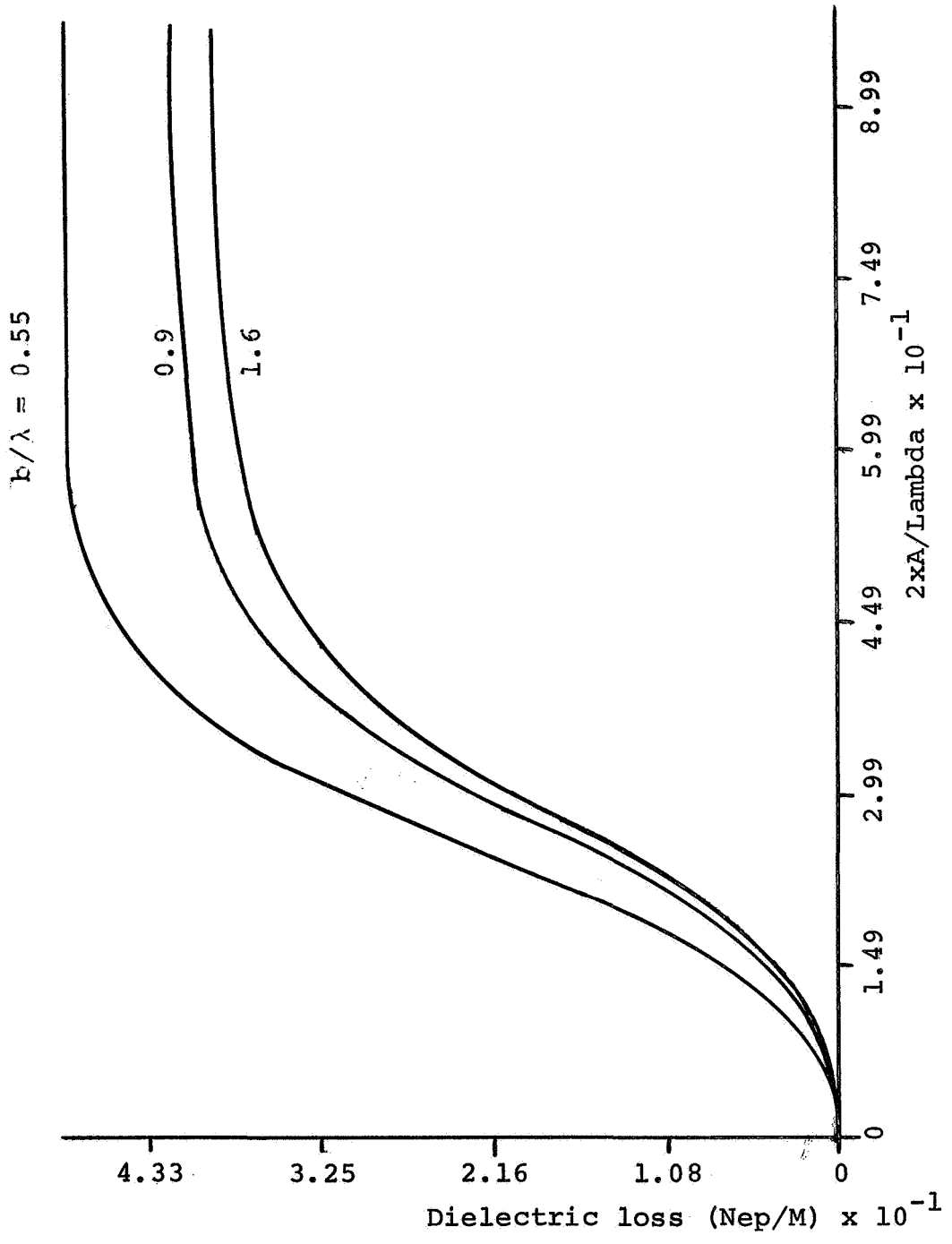

Fig. 6 Attenuation due to dielectric losses for Rexolite

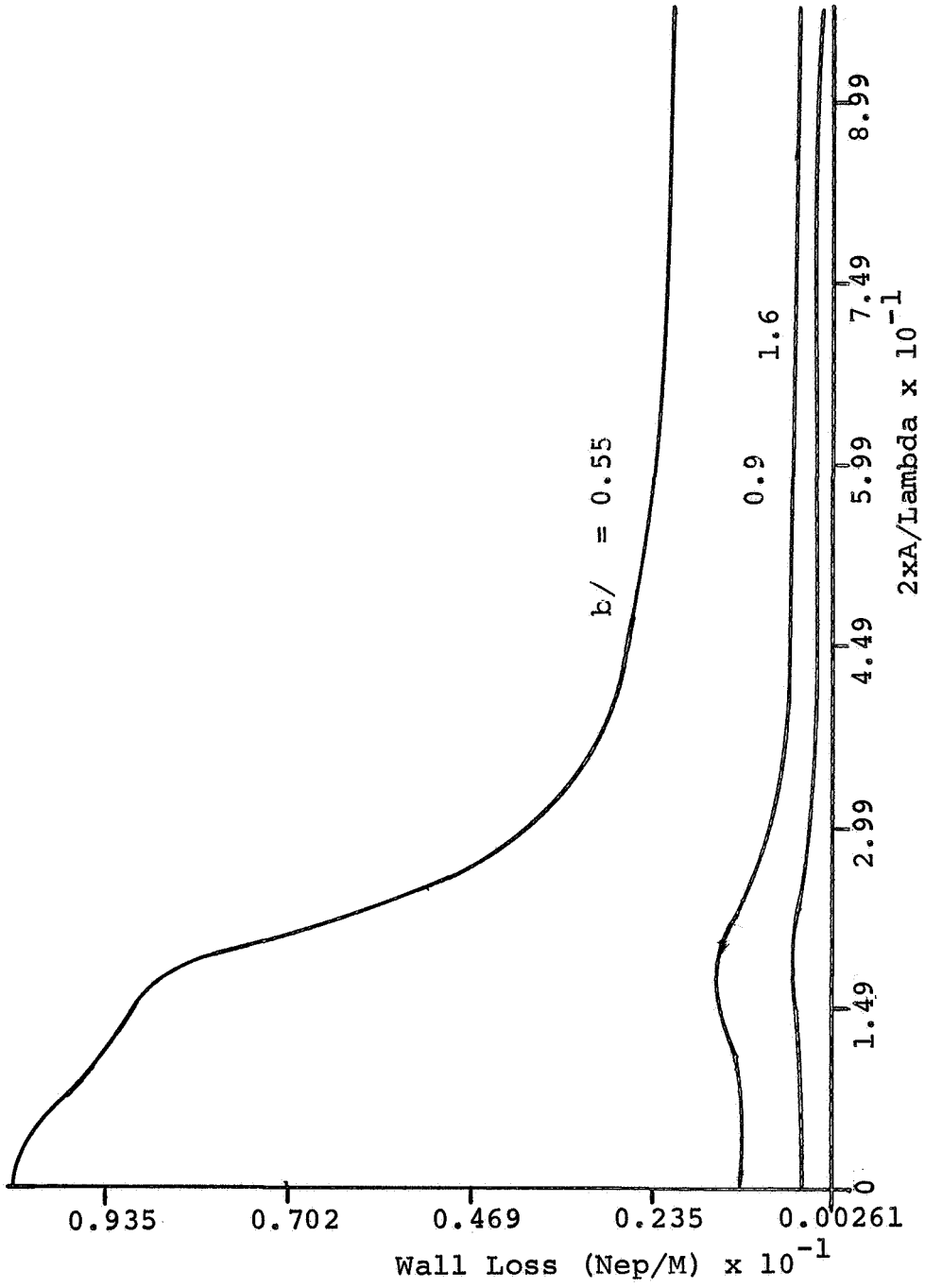

Fig. 7 Attenuation due to wall losses for a hypothetical dielectric
($\varepsilon_r = 6.0$, $\tan\delta = 5 \times 10^{-4}$)

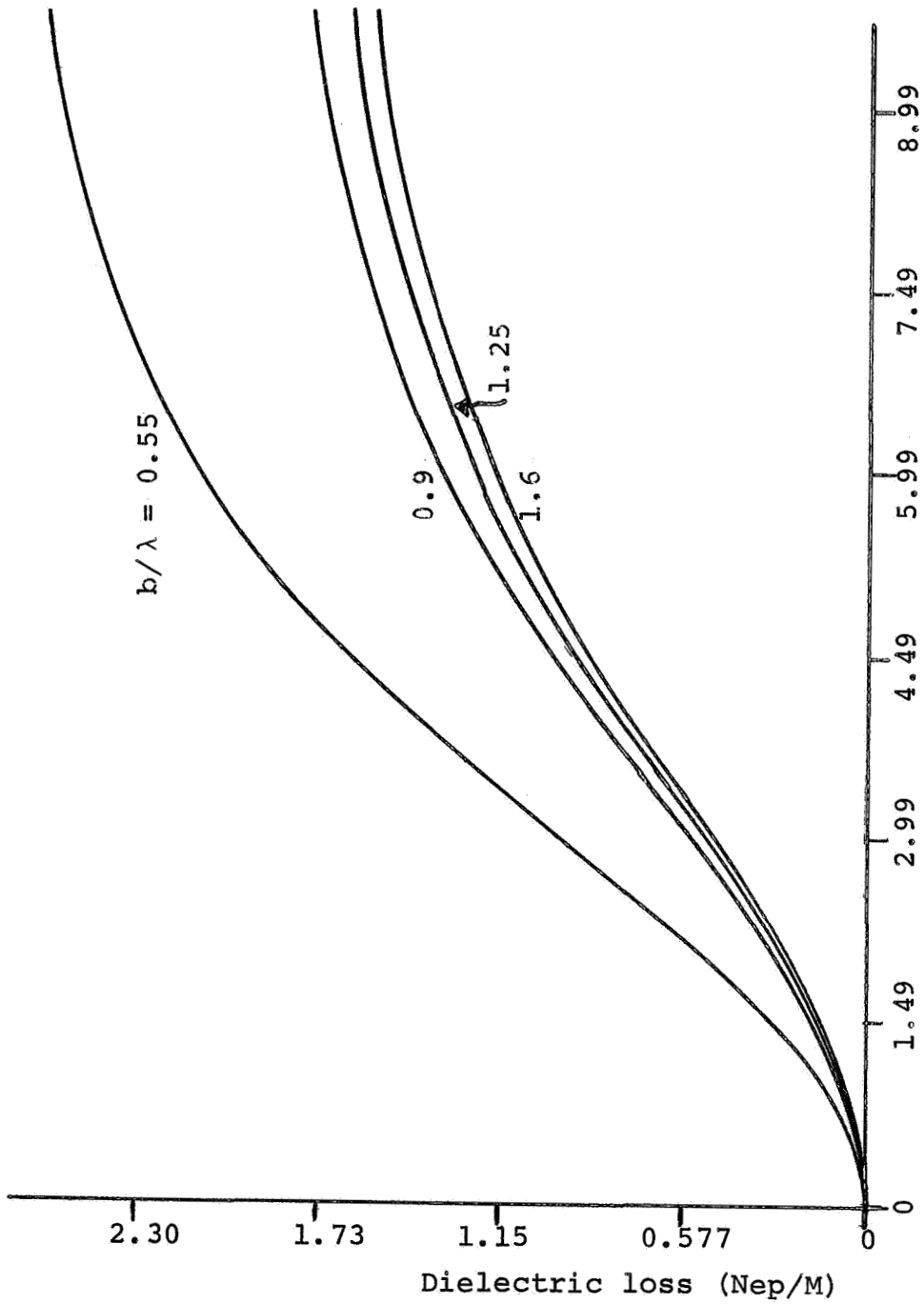

Fig. 8 Attenuation due to dielectric losses for hypothetical dielectric (see Fig. 6)

Program for Data Evaluation

DHGYD #2

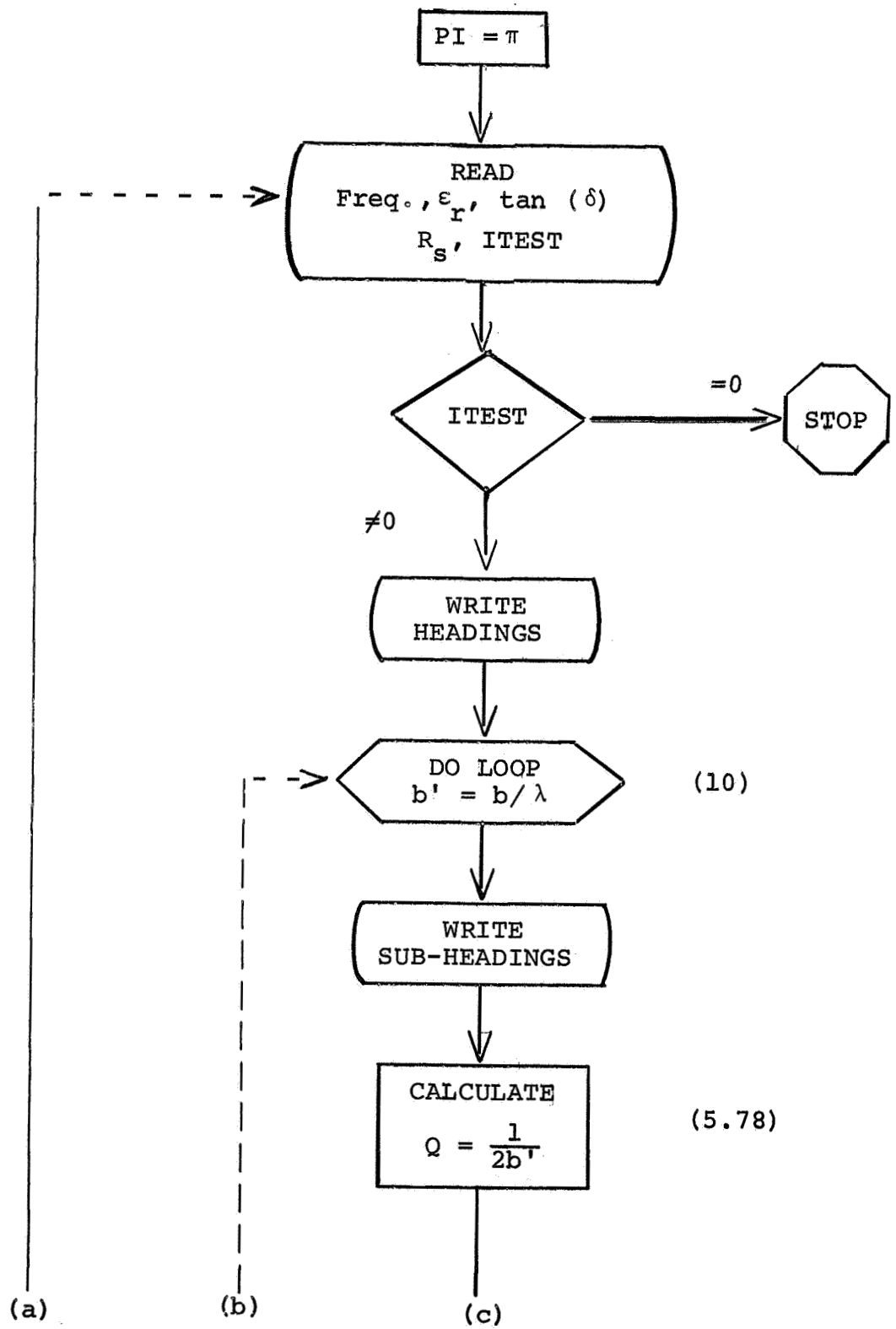

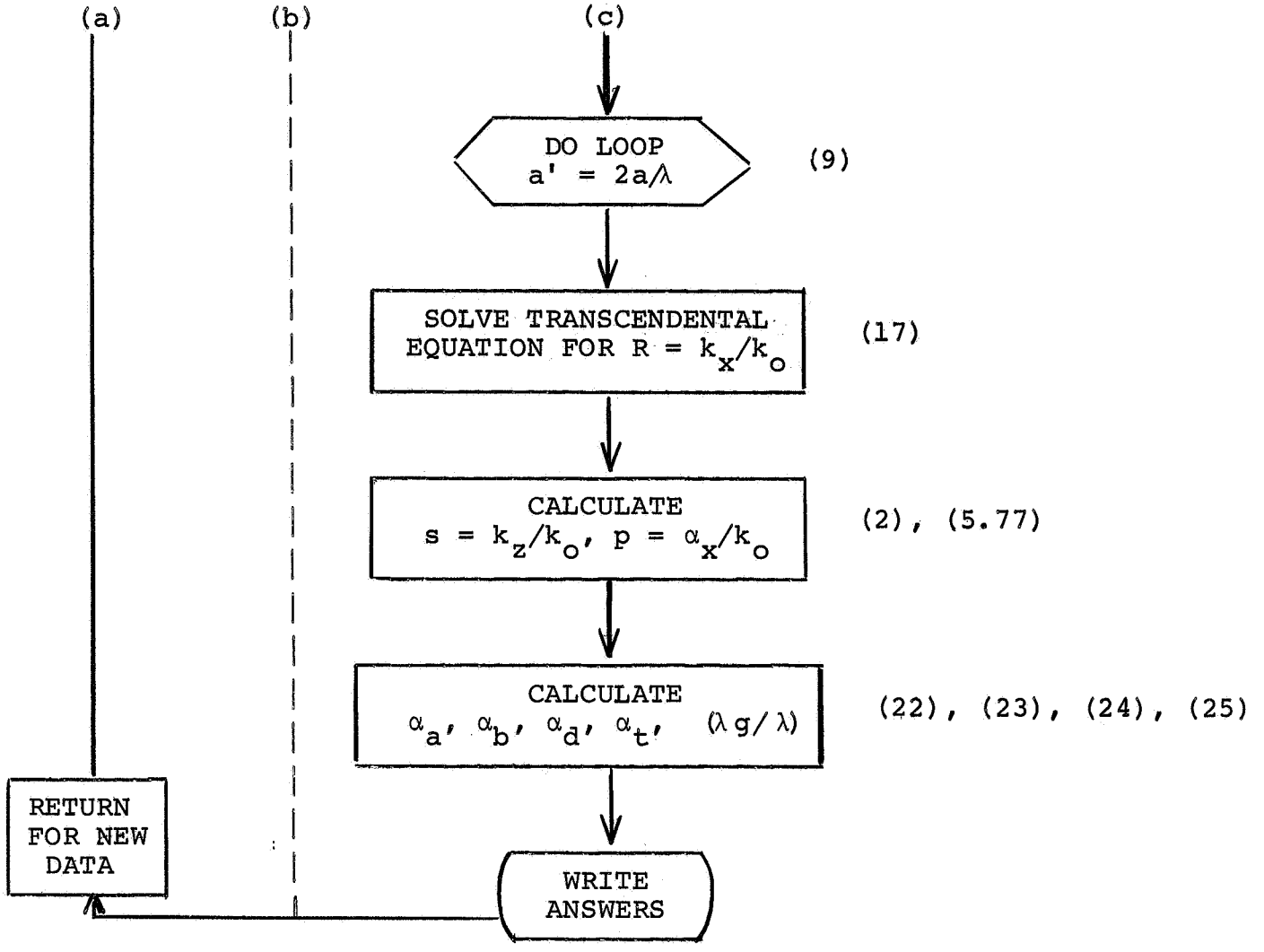
(a)
(b)
(c)
DO LOOP
a' = 2a/λ
(9)
SOLVE TRANSCENDENTAL EQUATION FOR R = k_x/k_o
(17)
CALCULATE
s = k_z/k_o, p = α_x/k_o
(2), (5.77)
CALCULATE
α_a, α_b, α_d, α_t, (λ g/ λ)
(22), (23), (24), (25)
WRITE ANSWERS
RETURN FOR NEW DATA

Computer Program for the Determination
of Guide Wavelength and Attenuation

```
OPTIONS      - NAME= DHG#3,OPT=02,LINECNT=56,SOURCE,EBCDIC,NOLIST
NODECK,LOAD,MAP,N
C    DIELECTRIC H-GUIDE  DHGYD#3
C    GRAPHS ATTENUATION AND GUIDE WAVELENGTH VS. SLAB THICKNESS
C    PROGRAM IDENTICAL TO DHGYD#2  EXCEPT FOR I/0
   IMPLICIT REAL*8(A-H,L,O-Z)
   REAL EPS,X1(40),X2(40),X3(40),X4(40),X5(40),X6(40),
  *         Y1(40),Y2(40),Y3(40),Y4(40),Y5(40),Y6(40),
  *         Y7(40),Y8(40),Y9(40),Y10(40),Y11(40),Y12(40)
   REAL*8 ANAME(2)
   EXTERNAL FCT
   COMMON APR,ER,PI
   PI=3.141592653589793
C    GRAPH DIMENSIONS
   CALL SIZE(6.5,4.5)
C    READ DATA
 1 READ(1,101)F,ER,TANDL,R SO,ITEST,(ANAME(I),I=1,2)
C    IDENTIFICATION OF VARIABLES:
C    F=FREQUENCY (HZ)
C    ER=RELATIVE PERMITTIVITY
C    TANDL=LOSS TANGENT
C    RSO=SURFACE RESISTIVITY
C           (TO BE MULTIPLIED BY 1.E-7*SQRT(F))
C    ITEST=INDEX TO MARK END OF DATA (ITEST=0 MEANS END OF DATA)
C   TEST FOR END OF DATA
   IF (ITEST) 3,2,3
 2 CALL PICSIZ(0.,0.)
   CALL EXIT
C    BEGIN DO LOOP.  PLATE SEPARATION (BPR=B/LAMBDA) VARIES
C                    0.55 TO 2.3 BY 0.35*LAMBDA
 3 DO 1001 I=1,6
   BPR=0.55+0.35*(I-1)
C    FIND Q=KY/KO:
C    KY=SEPARATION CONSTANT ACROSS GUIDE (=PI/B)
C    KO=FREE SPACE PROPAGATION CONSTANT (=OMEGA/C)
   Q=1./(2.*BPR)
C    INITIALIZE INDEX:  USED TO DETERMINE NUMBER OF POINTS
C    IN EACH CURVE AND FOR SUBSCRIPTS IN ARRAYS.
   JJ=0
C    BEGIN DO LOOP.  DIELECTRIC SLAB THICKNESS (APR=2*A/LAMBDA)
C                    VARIES 0.0 TO 0.975 BY 0.025*LAMBDA
   DO 1001 J=1,40
   APR=0.025*(J-1)
C    SOLVE TRANSCENDENTAL EQUATION FOR R=KX/KO.
C    KX=SEPARATION CONSTANT WITHIN DIELECTRIC.
   IF (APR) 11,10,11
 10 R=DSQRT(ER-1.DO)
   GO TO 7
```

```
   11 RLI=0
      RRI=1./(4.*APR)
      EPS=1.E-6
    4 CALL DRIMI(R,RO,FCT,RLI,RRI,EPS,1000,IER)
      IF (IER-1) 7,5,6
C          SOLUTION NOT FOUND WITHIN 1.E-6 AFTER 1000 ITERATIONS.
C          INCREASE TOLERANCE AND TRY AGAIN.
    5 EPS=EPS*5.
      GO TO 4
C          SOLUTION LIES TO RIGHT OF RRI.
C          MOVE RIGHT LIMIT HALF-WAY TOWARD SINGULARITY AND TRY AGAIN.
    6 RRI=RRI+((1./(2.*APR)-RRI)/2.)
      GO TO 4
C          R DETERMINED. TEST FOR OPERATION BELOW CUTOFF.
    7 ARG = ER-R*R-Q*Q
      IF (ARG) 8,8,9
C          BELOW CUTOFF.  INCREASE JJ BY 1 TO INDICATE THIS POINT
C          WILL NOT BE PLOTTED.
    8 JJ=JJ+1
      GO TO 1001
C          ABOVE CUTOFF.  CALCULATE S=KZ/KO.
C          KZ=PROPAGATION CONSTANT IN GUIDE.
C     1/S=(GUIDE WAVELENGTH)/(FREE SPACE WAVELENGTH)
    9 S=DSQRT(ARG)
      IF (APR) 13,12,13
   12 P=0.0
      GO TO 14
C          DETERMINE NORMALIZED DECAY CONSTANT. P=ALPHA-X/KO.
C          ALPHA-X=EXPONENTIAL DECAY CONSTANT IN AIR.
   13 P=DSQRT(Q*Q+S*S-1.DO)
C          PROGRAMMING AIDS
   14      H=PI*APR*(R*R+ER*ER*P*P)
           AA=RSO*F*DSQRT(F)*ER/1.8D17/PI/BPR*Q*Q/(1.DO+P*P)/
     *        (H*P+ER*(ER-1.DO))/S
           BB=AA*2.DO
C          CALCULATE ATTENUATION CONSTANTS (NEPERS PER METER)
C          WALL LOSSES, AIR REGION
      ALPHA=AA*(ER-1.DO-P*P)
C          WALL LOSSES,DIELECTRIC REGION
      ALPHA=AA*P*(H+ER*P)
C          DIELECTRIC LOSSES
      ALPHD=TANDL*PI*F*ER*P*(H*P+P*(2.DO-ER+2.DO*P*P))/
     *       (3.D8*S*(H+ER*(ER=1.DO)))
C          WALL LOSSES
      ALPHT=ALPHA+ALPHB
C          DIELECTRIC LOSSES
      LDGOL=ALPHD
C          STORE ARRAYS FOR GRAPHING
      GO TO (51,52,53,54,55,56),I
```

```
   51 X1(J-JJ)=APR
      Y1(J-JJ)=ALPHT
      Y7(J-JJ)=LDGOL
      N1=40-JJ
      GO TO 1001
   52 X2(J-JJ)=APR
      Y2(J-JJ)=ALPHT
      Y8(J-JJ)=LDGOL
      N2=40-JJ
      GO TO 1001
   53 X3(J-JJ)=APR
      Y3(J-JJ)=ALPHT
      Y9(J-JJ)=LDGOL
      N3=40-JJ
      GO TO 1001
   54 X4(J-JJ)=APR
      Y4(J-JJ)=ALPHT
      Y10(J-JJ)=LDGOL
      N4=40-JJ
      GO TO 1001
   55 X5(J-JJ)=APR
      Y5(J-JJ)=ALPHT
      Y11(J-JJ)=LDGOL
      N5=40-JJ
      GO TO 1001
   56 X6(J-JJ)=APR
      Y6(J-JJ)=ALPHT
      Y12(J-JJ)=LDGOL
      N6=40-JJ
 1001 CONTINUE
C          SET UP TITLE AND AXIS LABELS, AND DRAW TWO GRAPHS.
      CALL LABEL ('2*A/LAMBDA_','WALL LOSS(NEP/M)_',ANAME(1))
      CALL GRAPH(X1,Y1,N1,X2,Y2,N2,X3,Y3,N3,X4,Y4,N4,X5,Y5,N5,
                 X6,Y6,N6)
      CALL LABEL('2*A/LAMBDA_','DIELECTRIC LOSS(NEP/M)_',ANAME(2))
      CALL GRAPH(X1,Y7,N1,X2,Y8,N2,X3,Y9,N3,
     *           X4,Y10,N4,X5,Y11,N5,X6,Y12,N6)
C          RETURN FOR NEW DATA
      GO TO 1
  101 FORMAT(4D10.0,I2,2(2X,A8))
  102 FORMAT('1','NO.PTS.=',I3/'0','X (2*A/LAMBDA)',
     *5X,'Y(ALPHA)',9X,'Y(LAMBDA)'/)
  103 FORMAT(' ',3(D15.8,2X))
      END
```